



Degree Project in Electric Power Engineering

Second cycle, 30 credits

Implementation of Probabilistic Risk Assessment in the Short-Term Operational Planning at the Swedish National Grid

SIGNE AXÉN

Implementation of Probabilistic Risk Assessment in the Short-Term Operational Planning at the Swedish National Grid

SIGNE AXÉN

Master's Programme, Electric Power Engineering, 120 credits
Date: July 9, 2024

Supervisors: Arvid Rolander, Ebrahim Shayesteh

Examiner: Lars Nordström

School of Electrical Engineering and Computer Science

Host company: Svenska Kraftnät

Swedish title: Implementering av sannolikhetsbaserad riskbedömning i kortsiktig driftsplanering på Svenska Kraftnät

Abstract

Probabilistic Risk Assessment is a method in operational security management for power systems which offers transmission system operators a framework to assess the probability and impact of system failures, thus establishing operational security limits. Unlike the traditional, deterministic N-1 criterion, Probabilistic Risk Assessment incorporates the probability of disturbances, providing a more nuanced understanding of system vulnerabilities. The Probabilistic Risk Assessment methodology, required by Methodology for Coordinating operational Security Analysis Article 44 for implementation by 2027, mandates transmission system operators to consider uncertainties such as weather conditions and generation variability. This thesis explores the development and implementation of the Probabilistic Risk Assessment methodology for short-term operational planning within the Swedish transmission system operator, Svenska Kraftnät. It utilizes the VAFFEL-method, developed by Statnett, for forecasting probabilities of transmission line failures using Bayesian updating, reanalysis data, and medium-range weather forecasts. Compared to other Nordic and Baltic countries, Sweden has a high share of Energy Not Served due to lightning and unknown causes, leading to the focus on wind and lightning as key weather factors. The objectives are to evaluate the method's applicability to Swedish transmission system operator's operational practices, assess the need for additional data, identify potential improvements in data quality and quantity, and validate the method's relevance for Swedish transmission system operator. The research methodology involves a literature review, stakeholder consultations, data collection, pre-processing, testing, and validation. The existing VAFFEL-method by Statnett is adapted for Swedish conditions, incorporating data pre-processing algorithms and including lightning as a weather factor. Model accuracy is measured using Brier Score. Results indicate that the Swedish transmission system operator has sufficient data for the model to provide relevant outputs. Brier Score shows higher accuracy for the model's forecasted probabilities than for a constant failure rate, and also higher accuracy for predictions of failures due to wind than lightning, which however needs to be validated with a larger data set.

Keywords

Probabilistic Risk Assessment, Grid Contingencies, Transmission Grid, Short-term Operational Planning, Bayesian Statistics, Fragility Curve

Sammanfattning

Sannolikhetsbaserad riskbedömning är en metod inom driftsäkerhetshantering för elsystem som erbjuder transmissionsnätsoperatörer ett ramverk för att bedöma sannolikheten och konsekvenserna av systemfel och därigenom fastställa driftssäkerhetsgränser. Till skillnad från det traditionella, deterministiska N-1-kriteriet, inkluderar sannolikhetsbaserad riskbedömning sannolikheten för störningar, vilket ger en mer nyanserad bild av systemets sårbarheter. Metodologin för sannolikhetsbaserad riskbedömning, som enligt CSAM Artikel 44 ska implementeras senast 2027, förpliktar transmissionsnätsägare att beakta osäkerheter såsom väderförhållanden och variationer i produktion.

Detta examensarbete utforskar utvecklingen och implementeringen av metodologin för sannolikhetsbaserad riskbedömning för kortiktig driftplanering inom Svenska Kraftnät. Den använder VAFFEL-metoden, utvecklad av Statnett, för att förutsäga sannolikheter för transmissionsledningsfel med hjälp av en Bayesiansk metod, historisk väderdata och medellånga väderprognoser. Jämfört med andra nordiska och baltiska länder har Sverige en hög andel icke levererad energi på grund av blixtnedslag och okända orsaker, vilket motiverar fokus på vind och åska som viktiga väderfaktorer.

Målen är att utvärdera metodens tillämpbarhet på Svenska Kraftnäts operativa rutiner, bedöma behovet av ytterligare data, identifiera potentiella förbättringar i datakvalitet och -kvantitet samt att validera metodens relevans för Svenska Kraftnät.

Metodiken innefattar en litteraturöversikt, samråd med intressenter, datainsamling, bearbetning av data, testning och validering. Den befintliga VAFFEL-metoden av Statnett anpassas för svenska förhållanden, inklusive algoritmer för datapreparering och införande av åska som väderfaktor. Modellens noggrannhet mäts med Brier Score.

Resultaten visar att Svenska Kraftnät har tillräcklig data för att modellen ska ge relevanta resultat. Brier Score indikerar högre noggrannhet för modellens prognosticerade sannolikheter än för en konstant felfrekvens. Brier Score visar högre noggrannhet för förutsägelser av fel på grund av vind än på grund av åska, vilket dock måste valideras med ett större dataunderlag.

Nyckelord

Sannolikhetsbaserad Riskbedömning, Transmissionsnät, Driftplanering, Bayesiansk Statistik, Sårbarhetskurva.

Acknowledgments

I would like to thank my supervisor, Ebrahim Shayesteh at Svenska Kraftnät (Svk), and my supervisor Arvid Rolander at KTH, for their guidance and support throughout this project. I would also like to thank my examiner, Lars Nordström at KTH, for his constructive critiques. Furthermore I would like to extend my gratitude to Statnett and to the entire team at Svk for their assistance and for providing the necessary resources and data for this study. The collaborative environment and the support from my colleagues have been greatly appreciated. Finally, I would like to thank all the other individuals at Svk who have contributed in various ways to the success of this project. Your help and support have been invaluable.

Stockholm, July 2024

Signe Axén

Contents

1	Introduction	1
1.1	Background	1
1.2	Problem	2
1.3	Purpose & Goals	2
1.4	Research Methodology	3
1.5	Delimitations	3
1.6	Structure of the thesis	4
2	Background	5
2.1	Probabilistic Risk Assessment	5
2.1.1	EU Regulations	6
2.1.2	ENTSO-E Working Group PRA	7
2.2	Reliability today and current practices at Svk	8
2.2.1	Current practices	8
2.2.2	Grid disturbance statistics	8
2.3	PRA methods	10
2.4	Summary	12
3	Methodology and method	13
3.1	Data Collection	14
3.1.1	Historical weather data	14
3.1.2	Grid topology	16
3.1.3	Failure statistics	17
3.2	Data pre-processing	17
3.2.1	Hardware/Software to be used	19
3.2.2	Algorithm to convert transmission line data	19
3.2.3	Algorithm to map the weather data to the tower coordinates	20

3.3	Probabilistic model & parameters	20
3.3.1	Main steps of model algorithm	20
3.3.2	Bayesian failure rates	21
3.3.3	Weather exposure	26
3.3.4	Fragility curves	27
3.3.5	Forecast of line failure probabilities	28
3.4	Reliability and validity assessment	30
4	Results and Analysis	33
4.1	Bayesian failure rates	33
4.2	Fragility curves	34
4.2.1	Single segment fragility curves	34
4.2.2	Full line fragility curves	35
4.3	Reliability and Validity Analysis	37
4.3.1	Hourly probabilities of failure	37
4.3.2	Historical failures due to wind	38
4.3.3	Historical failures due to lightning	39
4.3.4	Mismatches between failures and predictions	41
4.3.5	Forecasted probabilities of failure	43
4.3.6	Brier Score	45
5	Discussion	47
6	Conclusions and Future work	49
6.1	Conclusions	49
6.2	Limitations	50
6.3	Future work	50
6.3.1	Set up the forecasting part	50
6.3.2	Validation of the model on an aggregated scale	50
6.3.3	Including more components and factors	51
6.3.4	In depth comparison to other forecasting models	51
References		53

List of Figures

3.1	An overview of the research methodology.	13
3.2	An overview of the main parts of the method.	14
3.3	Flowchart of the data pre-processing steps resulting in the final inputs for the model. The cylinder shapes are databases, the rectangular shapes are processes and the rectangles with waveshaped bottoms are documents.	18
3.4	Flowchart of the main parts of the model.	21
3.5	Overview of the process of computing fragility curves.	29
4.1	Comparison of fragility curves for lightning for different lines. Note that the scales on the y-axes are different due to different fragilities of the lines.	35
4.2	Comparison of fragility curves for wind for different lines. Note that the scales on the y-axes are different due to different fragilities of the lines.	35
4.3	Fragility curve K-index for Line A.	36
4.4	Fragility curve Total Totals-index for Line A.	36
4.5	Fragility curve wind for Line B.	36
4.6	Fragility curve wind for Line C.	36
4.7	Hourly probabilities of failure due to lightning 2012-2022. . .	37
4.8	Hourly probabilities of failure due to wind 2012-2022. . . .	37
4.9	Analysis of historical failures due to wind Line B coinciding with increased probability of failure.	39
4.10	Analysis of historical failure due to lightning Line A coinciding with increased probability of failure.	40
4.11	Analysis of historical failures due to lightning Line A coinciding with increased probability of failure.	40
4.12	Analysis of historical failures due to lightning Line A coinciding with increased probability of failure.	41

4.13 Analysis of historical failure wind Line B mismatched in time with increased probability of failure.	42
4.14 Analysis of historical failures due to lightning Line A mismatched in time with increased probability of failure.	42
4.15 Forecasted probabilities of failure on new data for 2023 Line A.	44
4.16 Forecasted probabilities of failure on new data for 2023 Line B without actual failure occurring.	44
4.17 Forecasted probabilities of failure on new data for 2023 Line C without actual failure occurring.	45
4.18 Comparison of Brier Scores for all three lines including constant failure rate, wind and lightning modelling.	46

List of Tables

2.1	Percentage allocation of grid disturbances by cause over 2013–2022. Proportionately higher percentage values are highlighted in yellow and red [8].	9
2.2	Percentage allocation of grid disturbances that caused Energy Not Served (ENS) by cause over 2013–2022. Proportionately higher percentage values are highlighted in yellow and red [8].	10
3.1	K-index values and the corresponding potential for thunder-storm development [21].	16
3.2	Total Totals-index values and the corresponding probability and severity of thunderstorms [21].	16
3.3	Example of failure statistics	17
3.4	Example table describing the output file of the weather data processing script. Each weather parameter is presented in a separate sheet.	20
4.1	Prior and posterior failure rates for Line A,B and C based on failure statistics for 1998-2023. The priors are adjusted to the line lengths, which is why the priors are different between the lines, as they are of different lengths.	34

List of acronyms and abbreviations

ACER	European Union Agency for the Cooperation of Energy Regulators
CSAM	Methodology for Coordinating operational Security Analysis
ENS	Energy Not Served
ENTSO-E	European Network of Transmission System Operators for Electricity
GARPUR	Generally Accepted Reliability Principle with Uncertainty modelling and through probabilistic Risk assessment
GIS	Geographic Information System
PRA	Probabilistic Risk Assessment
RSC	Regional Security Coordinator
Svk	Svenska Kraftnät
TSO	Transmission System Operator
VAFFEL	VArsel Før FEiL

Chapter 1

Introduction

This chapter introduces the research topic by providing a brief background, outlining the problem statement, and defining the purpose and goals of the study. Additionally, it presents the structure of the thesis to guide the reader through the subsequent chapters.

1.1 Background

In Sweden and the rest of Europe, the management of power system operational security has traditionally depended on the N-1 criterion as the fundamental principle for contingency analysis. The N-1 criterion ensures that the power system can handle an unforeseen failure or outage of a single system component, adapt to the new operational conditions, and remain within established security limits.

Probabilistic Risk Assessment (PRA) is as a complementary method in the operational security management of power systems, offering Transmission System Operators (TSOs) a framework to evaluate the probability and impact of system failures when establishing operational security limits. This method complements the traditional N-1 criterion by incorporating the probability of various disturbances, thus providing a more nuanced understanding of system vulnerabilities [1]. The PRA methodology, mandated by European Union Agency for the Cooperation of Energy Regulators (ACER)'s Methodology for Coordinating operational Security Analysis (CSAM) Article 44 for implementation by 2027, requires TSOs to account for uncertainties such as weather conditions and generation variability [2].

The development of the PRA methodology is a collaborative effort by many European TSOs, coordinated by European Network of Transmission

System Operators for Electricity (ENTSO-E). Within ENTSO-E, a working group for PRA (WG PRA) includes participants from 16 TSOs and focuses on three different workstreams [1]. The first workstream is reporting and stakeholder management, the second is infrastructure and data collection, and the third is methodology and definition development. Within the third workstream, the Norwegian TSO Statnett has presented a methodology called VArsel Før FEiL (VAFFEL), which translates roughly to 'Warning For Failure,' with the main function of predicting hourly probabilities of failure for overhead lines [1]. The goal of this degree project is to contribute to the development of the PRA methodology and its implementation at the Svenska Kraftnät (Svk), by testing and adapting the above mentioned method.

1.2 Problem

The current process for short-term operational planning at Svk is deterministic and assumes that all failures have equal probability in the contingency analysis. To comply with EU regulations, Svk must implement a probabilistic method in short-term operational planning by 31 December 2027. The method development process is a collaborative effort led by ENTSO-E's working group on PRA, involving several European TSOs. Svk aims to take an active role in this development, which motivates this thesis project that investigates the current status and feasibility of implementing PRA in short-term operational planning.

Research questions:

- How can Svk implement PRA in short term operational planning to meet the requirements in EU regulations?
- Is the VAFFEL-method developed by Statnett a feasible method to implement at Svk, and what is needed in order to do that?
- Is there sufficient data available today at Svk to use the VAFFEL-method?

1.3 Purpose & Goals

The purpose of this thesis project is to investigate how Svk can implement PRA in short term operational planning based on the VAFFEL-method and if there is sufficient data available today to start implementation. The goals of this thesis project are to:

- Identify how the VAFFEL-method can be incorporated in existing internal operational processes
- Identify the data required for using the method and whether Svk has a sufficient data availability today to produce relevant results with the method.
- Identify how the existing data collection can be improved in terms of quality and quantity, to produce more accurate results.
- Test the model with Svk data
- Identify how the VAFFEL-method can be extended or adjusted to bring maximum value at Svk, in accordance with the requirements by ACER in CSAM.

1.4 Research Methodology

The research methodology in this project includes two main parts. The first part aims to gather previous experience and knowledge on the subject and includes a literature review and discussions with relevant experts both internally at Svk and at other TSOs. The second part of the methodology aims to investigate the practical implementation feasibility of the PRA model, including collecting and pre-processing data, and testing and validating the model. The motivation behind choosing to investigate the feasibility of the VAFFEL-method specifically, instead of another method or developing a new one, is that it was suggested by ENTSO-E as an available and suitable method to test.

1.5 Delimitations

The scope of this thesis project is limited to the short-term operation planning perspective, of PRA and does not include methods for medium or long-term planning. Short-term is in this work defined as up to a couple of days ahead. The project focuses on assessing the possibility of implementing the VAFFEL method at Svk and does not provide an in-depth comparison to other methods. This work does not include any assessment of the consequences of failure, only the probability. Regarding components and weather factors, the only component included is overhead lines, and the weather factors considered are wind and lightning.

1.6 Structure of the thesis

Chapter 2 presents background information about PRA, the legal obligations according to EU regulations and previous related work. Chapter 3 presents the method including data collection, data pre-processing and the investigated PRA-model. Chapter 4 presents the results and analysis, including an evaluation of validity and reliability. Lastly discussion of the results, conclusions and future work are presented in chapter 5 and 6.

Chapter 2

Background

This chapter provides basic background information about probabilistic risk assessment, the legal obligation of all TSOs to implement it, and the ongoing working structure set up by ENTSO-E. Additionally, this chapter describes the current practices at Svk and the reliability of the Swedish grid today. Furthermore, the chapter discusses previous work in the area, including the VAFFEL methodology, and other methods.

2.1 Probabilistic Risk Assessment

Probabilistic Risk Assessment (PRA) is a methodology employed to quantitatively evaluate and analyze the likelihood of diverse outcomes or scenarios within a given system. In contrast, N-1 represents a deterministic criterion utilized to ensure system resilience, stipulating that the system can withstand the failure of a single component without compromising operational security [3] [1].

PRA is a broad subject and can be applied in different ways, for different parts of the transmission system and over various time-periods. By accounting for various uncertainties, including component failures and external events, PRA facilitates the identification of vulnerabilities and informs prioritization of risk mitigation strategies [3] [1]. Through the quantitative assessment of different scenarios, PRA empowers decision-makers to make informed choices regarding system operation, maintenance, and investment, ultimately enhancing system resilience and reliability. This thesis will only explore a part of the subject as a whole.

Earlier work on the theme includes a larger EU-funded project Generally Accepted Reliability Principle with Uncertainty modelling and through

probabilistic Risk assessment (GARPUR) conducted between 2013-2017, involving 7 European TSOs and several other actors [3]. The project aimed at designing, developing and assessing new reliability criteria to implement gradually over the coming decades at a European level. The goal of the new reliability criteria included minimizing socio-economic cost, by operating the power systems efficiently [3]. The scope of GARPUR covered areas such as system operation, asset management, system development and focuses both on probability and consequence aspects of contingencies in the power system [3]. A probabilistic approach in power system operation has been examined and supported by earlier work as well, showing advantages over the deterministic approach [4].

2.1.1 EU Regulations

This section gives a brief overview of the legal obligations of the European TSOs to implement PRA methodology.

2.1.1.1 ACER

ACER is a regulatory body with the role of ensuring the effective functioning of Europe's single energy market [5]. ACER facilitates cooperation among national regulatory authorities at the EU level and oversees the implementation of energy regulations and guidelines, including those pertaining to system operation and market integration [5].

2.1.1.2 SO regulation

Methodology for coordinating operational security analysis (CSAM) is a comprehensive framework that integrates general principles and objectives set forth in Article 75 in Commission Regulation (EU) 2017/1485, established on 2 August 2017 [2] [6]. This regulation, commonly referred to as the System Operation (SO) Regulation, establishes guidelines for the secure and efficient operation of the electricity transmission system in Europe [6]. It outlines responsibilities and procedures for Transmission System Operators (TSOs) to maintain system security and reliability, particularly under contingency scenarios. The regulation mandates the development and implementation of various methodologies and practices to ensure coordinated and harmonized system operation across member states [2] [6].

2.1.1.3 Methodology for coordinating operational security analysis (CSAM)

The implementation of PRA methodology for all European TSOs is legally mandated in CSAM Article 44, which states that the implementation should be started latest December 2027 [2].

Article 44, Towards probabilistic risk assessment, paragraph 3-5 of CSAM states that:

- By nine months after the adoption of the CSAM, all TSOs must identify and collect data necessary for developing operational probabilistic coordinated security assessment and risk management. This process should be reviewed as needed based on the findings of related reports and the approved methodology on common probabilistic risk assessment [2].
- By 31 December 2027, all TSOs must jointly develop the methodology on common probabilistic risk assessment, considering the requirements of Article 75(1)(b) and Article 75(5) of the SO Regulation. This methodology should be proposed as an amendment to the existing methodology and, after approval, will become an annex to the original methodology [2].
- All TSOs and Regional Security Coordinators (RSCs), with the support of ENTSO-E, must establish the operational processes and infrastructure required to collect and process the necessary data by 21 months after the adoption of the CSAM [2].

2.1.2 ENTSO-E Working Group PRA

Based on the legal obligation described in Section 2.1.1, ENTSO-E formed a working group for PRA with the main goal of developing a PRA methodology by 2027. The latest progress of the PRA working group was published in December 2023 in the Biennial Progress Report on Operational Probabilistic Coordinated Security Assessment and Risk Management [1]. The PRA working group focuses on three main workstreams, with workstream 3 dedicated to developing the methodology for PRA. Challenges outlined in the report include ensuring that the developed methodology is consistent with the legal mandate while balancing practicality, complexity, network security, and socioeconomic value [1].

Within the working group, Statnett has presented the VAFFEL method as a potential tool for implementing PRA in short-term operational planning. The tool, described in more detail in Section 2.3, is currently being tested operationally within Statnett [1].

2.2 Reliability today and current practices at Svk

The aim of this section is to provide an overview of current practices at Svk and to identify the conditions in Sweden that might differ from those in other countries.

2.2.1 Current practices

Currently the operation and short term operational planning at Svk is done without input of the probability of different failures. A contingency analysis is performed where all consequences of different line failure are considered [7]. All failures are treated as equally probable, according to the historic deterministic N-1 criterion. Possible negative consequences of not distinguishing probabilities of failure are cause of unnecessary safety margins in for example capacity allocation which does not allow operation in the most economical and efficient way [7]. The conclusion regarding the current practices is that they are not in line with the goals of CSAM, however there are possible openings for starting implementation of probabilistic trials in the operation, for example as a complement in the contingency analysis.

2.2.2 Grid disturbance statistics

The latest statistics on grid disturbances in the Nordic and Baltic grid were published in October 2023, summarizing the year 2022. The statistics show that, compared to other countries in the region, Sweden has a larger share of the Energy Not Served (ENS) caused by lightning [8].

The total ENS caused by grid disturbances in Sweden was 650 MWh in 2022, compared to the 10-year annual average of 1343 MWh ENS. There were 426 grid disturbances, compared to a 10-year annual average of 438, with 158 causing ENS [8].

The main component causing ENS in Sweden during 2022 was overhead lines, accounting for 57% of the total ENS, followed by substations at 27%.

The most significant sources of ENS caused by disturbances were lightning (54%) and other causes (25%). Among all disturbances, both those leading to ENS and those not recorded as causing ENS, 35% were due to unknown reasons and 31% were due to lightning. Secondary faults accounted for 2% of all faults and did not cause any ENS [8].

Notably, the statistics reveal a high share of faults due to unknown reasons, indicating an area for improvement in future data collection.

Several specifically mentioned disturbances occurred on overhead lines, particularly on transmission towers, primarily caused by damaged parts due to strong winds and the natural wear and tear associated with an aging transmission network [8].

The grid components that caused the largest share of ENS in 2022 were overhead lines in Finland (99%), Iceland (59%), Sweden (57%), Lithuania (56%), and Norway (45%). In Estonia, it was circuit breakers (91%), in Latvia control equipment (74%), and in Denmark busbars (49%) [8].

Table 2.1: Percentage allocation of grid disturbances by cause over 2013–2022. Proportionately higher percentage values are highlighted in yellow and red [8].

Country	Lightning	Other environmental causes	External influences	Operation and maintenance	Technical equipment	Other	Unknown
Estonia	10%	22%	8%	14%	25%	12%	8%
Latvia	10%	25%	24%	6%	9%	9%	17%
Lithuania	7%	6%	26%	7%	6%	15%	33%
Denmark	8%	11%	22%	19%	20%	12%	9%
Finland	20%	32%	2%	6%	4%	17%	19%
Iceland	3%	38%	2%	9%	13%	32%	3%
Norway	19%	34%	2%	14%	19%	8%	4%
Sweden	36%	4%	2%	7%	13%	11%	28%

Table 2.1 shows a comparison of the causes of grid disturbances over the years 2013-2022 between the different countries. The figure shows that lightning is a more common cause for grid disturbances in Sweden compared to other countries.

Table 2.2 shows a similar comparison of ENS distributed over different causes. The same pattern is visible here, where Sweden stands out with a high share of ENS caused by lightning compared to other countries.

It is important to note that the relatively high share of faults and ENS caused by unknown faults, which has to be considered. For example it is unknown how large the share of wind-related grid disturbances is in reality, since this could be under-reported.

Table 2.2: Percentage allocation of grid disturbances that caused ENS by cause over 2013–2022. Proportionately higher percentage values are highlighted in yellow and red [8].

Country	Lightning	Other environmental causes	External influences	Operation and maintenance	Technical equipment	Other	Unknown
Estonia	3%	9%	10%	26%	21%	24%	8%
Latvia	2%	33%	26%	17%	13%	7%	3%
Lithuania	4%	10%	41%	24%	11%	4%	7%
Denmark	3%	8%	0%	49%	25%	10%	5%
Finland	16%	16%	3%	10%	7%	14%	34%
Iceland	4%	51%	2%	11%	14%	18%	1%
Norway	25%	26%	2%	20%	16%	7%	3%
Sweden	39%	2%	2%	8%	12%	10%	27%

2.3 PRA methods

The Norwegian TSO, Statnett, has developed a tool for forecasting transmission line failures based on Bayesian updating, reanalysis data and medium range weather forecasts [9] [10]. The tool is named VAFFEL, an acronym for "Varsel For Feil", which translates to "Warning ahead of failure". The tool is currently being tested operationally within Statnett. The components currently included in the analysis are overhead lines and the weather factors included are wind and lightning. In Norway wind is the largest cause of ENS [11].

The method uses a combination of previous failure statistics for the given transmission lines, historical weather data and a Bayesian updating scheme to create fragility curves describing the correlation between weather exposure and probability of failure for the given transmission line. The fragility curves can then be used in combination with a medium range weather forecast to create a prognosis of probability of failure for every line and hour [11].

Various other methods for PRA are found in the literature, with focus on slightly different areas. As for PRA methods focused on long term planning, a comparison can be found in the master thesis [12]. This thesis project is however limited to short term operational planning, which will be the focus forward on.

Regarding PRA implementations in short term operational planning, methods suggested are based on Markov chain models [13], different machine learning models such as Support Vector Machine and Boosting Trees [14] [15], Bayesian deep learning [16], Bayesian networks [17], different probability distributions [18] and big data platforms [19]. The use of fragility curves are found in [20] [16].

Markov chain models are praised for their predictive power and ability

to model the probabilistic transitions between different states of the system, effectively capturing time-dependent behavior of system components [13]. However, they are complex to implement and require detailed modeling of state transitions, which can be data-intensive. Additionally, they rely on the assumption that future states depend only on the current state, which may not always hold true.

Machine learning models, such as Support Vector Machine and Boosting Trees, are known for achieving high predictive accuracy with appropriate training data and their flexibility in modeling non-linear relationships and interactions in the data [14] [15]. Nevertheless, these models require large amounts of high-quality data for training and can be difficult to interpret due to their black box nature.

Bayesian deep learning offers significant advantages in uncertainty quantification and adaptability, providing estimates of uncertainty along with predictions and adapting to new data through continuous learning [16]. The main drawbacks are the significant computational resources required for training and inference and the complexity of implementation and understanding compared to simpler models.

Bayesian networks are capable of modeling causal relationships between variables and can handle large, complex systems with many interacting components [17]. However, they require detailed knowledge of the system to construct the network accurately and their performance is highly dependent on the quality and completeness of the input data.

Using different probability distributions for PRA is straightforward and based on well-established statistical principles, making it simple to understand and implement [18]. However, this approach may not capture complex interactions or non-linearities in the data and often relies on assumptions about the underlying distributions that may not hold true.

Fragility curves are useful for assessing the probability of failure under different stress conditions and provide a clear, visual representation of risk [20] [16]. They require detailed historical data to construct accurate curves and are specific to the components and conditions they are derived from, which may limit their generalizability to other scenarios.

Each of these methods offers unique advantages and faces specific challenges, underscoring the importance of selecting the appropriate method based on the specific requirements and constraints of the operational planning task at hand.

2.4 Summary

In summary, the conclusion from the pre-study is that the implementation of PRA in short-term operational planning at Svk is highly motivated by regulations. There is a gap between the expected status in the implementation timeline by ENTSO-E and the current status at Svk. A possible method to test and validate is the VAFFEL-method presented by Statnett. The Bayesian approach used in the VAFFEL-method allows for computing statistically plausible failure rates even for transmission lines without any recorded failures, which supports a potential implementation at Svk, even if the failure statistics are not complete. More than half of all the ENS in the Swedish transmission system is due to weather exposure, with lightning as the main cause. This motivates implementing the method for lightning as the primary weather factor. Other methods exist that are more or less related to the Bayesian statistical foundation in the VAFFEL-method, and these could be further investigated and compared to VAFFEL in future work.

Chapter 3

Methodology and method

The purpose of this chapter is to provide an overview of the research methodology and methods used in this thesis. An overview of the methodology is seen in Figure 3.1. The methodology consisted of an initial phase of gathering information about the problem, the current status, and possible methods by discussions with stakeholders, as well as a literature review. The second stage of the methodology was to test the model as decided during the previous stage and finally to analyze the results.

The method, connected to the later stages of the methodology, is illustrated in Figure 3.2, and consists of the main parts: data collection in section 3.1, data pre-processing in section 3.2, probability calculations in section 3.3, and validity assessment in section 3.4.

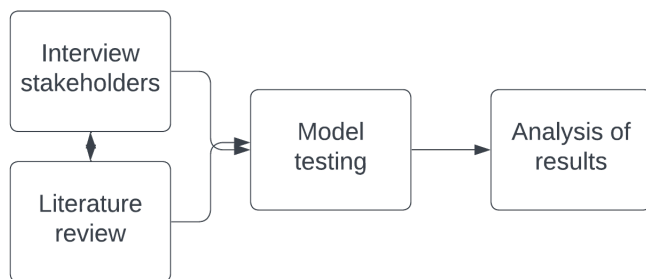


Figure 3.1: An overview of the research methodology.

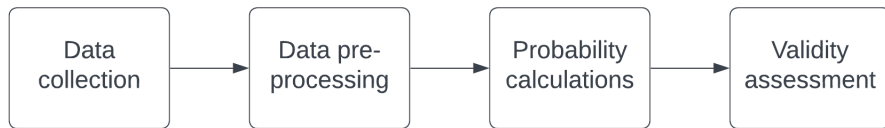


Figure 3.2: An overview of the main parts of the method.

3.1 Data Collection

The data collected as input for the model is historical weather data, grid topology and coordinates, and failure statistics. Both internal and external sources were used to gather data.

3.1.1 Historical weather data

Historical weather data was downloaded from Copernicus Climate Data Store via the CDS API client [21]. The dataset downloaded is *ERA5 hourly data on single levels from 1940 to present* where the variables *100m u-component of wind, 100m v-component of wind, K-index and Total Totals-index* are selected for the time period 2012-01-01 to 2023-12-31. ERA5 provides reanalysis data, which means a combination of model data and observations, resulting in hourly estimates of weather parameters in a latitude-longitude grid with a resolution of $0.25^\circ \times 0.25^\circ$ [21]. The geographical area of the downloaded data is selected to the coordinates corresponding to the borders of Sweden in North, South, East and West. The output file format chosen is netCDF4.

Input data to CDS API client:

start_datetime Start date and time for data retrieval (e.g., 2012-01-01).

end_datetime End date and time for data retrieval (e.g., 2023-12-31).

weather_data_types_ER5_single_levels List of weather data types to download:

- 100m_u_component_of_wind
- 100m_v_component_of_wind
- k_index

- total_totals_index

area Geographical area for data retrieval specified as [N, W, S, E] (e.g., [69, 10, 55, 25]). Coordinates are given in the WGS84 coordinate system.

3.1.1.1 Wind parameters

The 100m u-component of wind parameter represents the eastward horizontal speed component of air at an altitude of 100m above the earth surface given in meters per second. The altitude of transmission lines vary between ca 20 and 100 meters. The available heights in ERA5 are 10m and 100m, whereof 100m was chosen since it is closest to the transmission line height. The 100m v-component of wind parameter represents the equivalent in the northward direction. The two parameters are then combined in the model to give the total wind speed at each location [21]. A limitation of the wind-data extracted from the ERA5 dataset is that the actual local wind speed can differ from the given averages in the modeled weather grid due to local topography and terrain. The threshold indicating that wind is a factor relevant to consider as a cause of line failure is set to 15m/s [10]. Below the threshold the assumption is that any failure is not wind-related.

3.1.1.2 Lightning parameters

K-index is a parameter which indicates the potential for a thunderstorm to develop with a correlation as showed in Table 3.1 [21] [21]. The value is given in Kelvin and calculated as follows

$$K = (T_{850} - T_{500}) + D_{850} - (T_{700} + D_{700}) \quad (3.1)$$

where T_p is the temperature and D_p is the dew point temperature at pressure level p . The threshold value of the K-index in the model is set to 20 K, above which the probability of lightning is increased [21].

Total Totals-index is another parameter which also indicates the probability of a thunderstorm's occurrence and it's potential severity according to the correlation in Table [21]3.2 [21]. The threshold value of the Total Totals-index in the model is set to 45 K, above which the probability of lightning is increased. The value is given in Kelvin and is calculated as follows

$$TT = (T_{850} - T_{500}) + (D_{850} - T_{500}) \quad (3.2)$$

Both indices have limitations and strengths, which motivates using a combination of both in the model. A strength of the Total Totals-index in comparison to the K-index is that it includes an estimate of severity of the potential thunderstorm. Both indices are affected by geographical variations depending on the specific local conditions [21].

Table 3.1: K-index values and the corresponding potential for thunderstorm development [21].

K-index Value	Potential for Thunderstorm Development
< 20 K	No thunderstorm
20-25 K	Isolated thunderstorms
26-30 K	Widely scattered thunderstorms
31-35 K	Scattered thunderstorms
> 35 K	Numerous thunderstorms

Table 3.2: Total Totals-index values and the corresponding probability and severity of thunderstorms [21].

Total Totals-index Value	Probability and Severity of Thunderstorm
< 44 K	Thunderstorms not likely
44-50 K	Thunderstorms likely
51-52 K	Isolated severe thunderstorms
53-56 K	Widely scattered severe thunderstorms
56-60 K	Scattered severe thunderstorms more likely
> 60 K	Numerous severe thunderstorms

3.1.2 Grid topology

Grid data needed in order to calculate weather impact for specific transmission lines includes coordinates for each tower of the transmission line, line segment lengths and voltage levels. This data is collected from an internal Geographic Information System (GIS)-database at Svk and then converted into the right format. Three overhead lines are chosen based on diversity in geographical location and number of recorded faults due to wind and lightning respectively in the failure statistics. Line A has a relatively high occurrence of faults due to wind, Line B has a relatively high occurrence of faults due to lightning and Line C does not have recorded faults due to either wind or lightning during the selected time period.

3.1.3 Failure statistics

Disturbance statistics are extracted from an internal database at Svk and sorted, resulting in a table similar to the example in Table 3.3. The columns included in the model are the date and time of the failure, the component name, the type of the failure and the failure source. Only failures due to wind or lightning are extracted from the database. The type of the failure can be either temporary or permanent. A temporary fault does not require human intervention to be resolved and typically has a duration of seconds to minutes. A permanent fault on the other hand requires human intervention and typically last for hours to weeks. The duration of faults is not considered in the model beyond the information associated with the fault type.

Table 3.3: Example of failure statistics

Date_Time	Component	Type	Source
2000-07-03 13:51	Line A	Temporary	wind
2001-07-08 14:43	Line A	Temporary	wind
2002-07-17 11:13	Line B	Temporary	lightning
...
2011-07-31 15:38	Line A	Temporary	wind
2012-07-31 16:42	Line B	Temporary	lightning
...
2016-08-16 18:56	Line B	Temporary	lightning
2016-08-16 19:18	Line A	Temporary	lightning

3.2 Data pre-processing

Before the input data can be used in the model it is pre-processed as described in this section. A flowchart showing the pre-processing steps is seen in Figure 3.3.

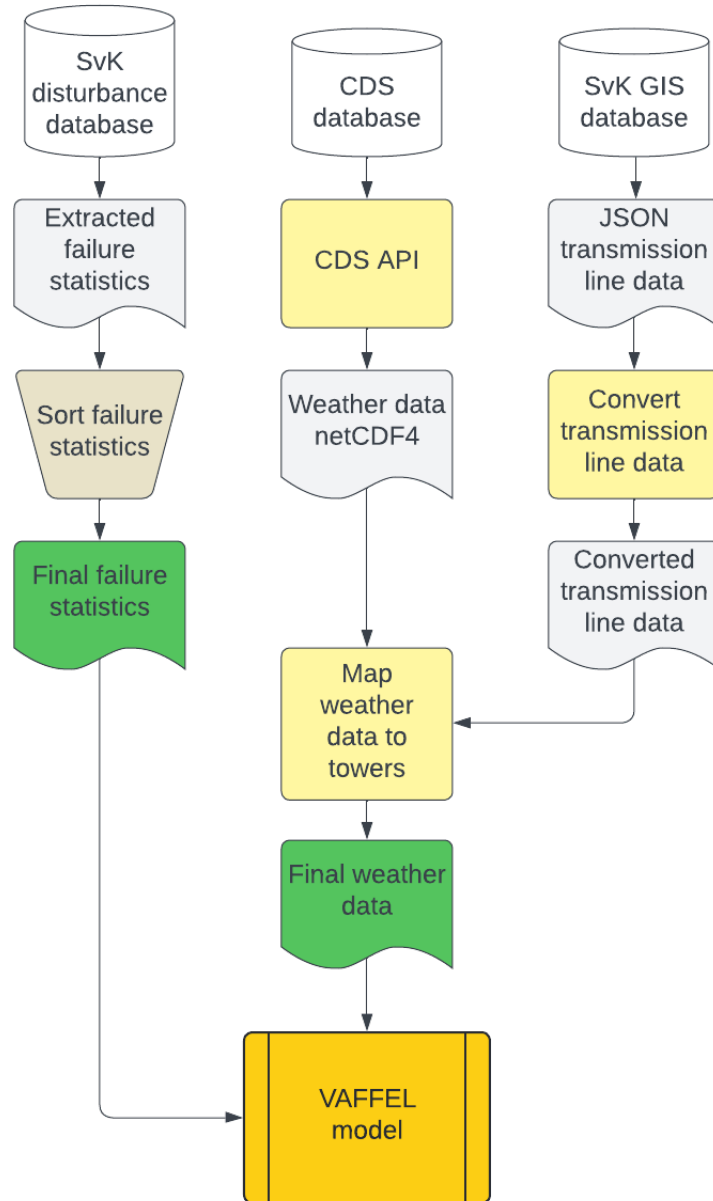


Figure 3.3: Flowchart of the data pre-processing steps resulting in the final inputs for the model. The cylinder shapes are databases, the rectangular shapes are processes and the rectangles with wavyshaped bottoms are documents.

3.2.1 Hardware/Software to be used

In this project, various software tools, programming environments and file formats were utilized to analyze and process the data. Here is a detailed list of the tools and resources employed:

Software and Programming Environments

- **Python:** The main programming language used for data processing and analysis.
- **Jupyter Notebook:** An interactive environment for running Python code, visualizing data, and documenting the analysis process.
- **Visual Studio Code (VSCode):** A code editor used for writing and debugging Python scripts.
- **CDS API client (Copernicus):** A service for accessing climate data from the Copernicus Climate Data Store.

File Formats

- **JSON:** JavaScript Object Notation, used for storing and exchanging data.
- **CSV:** Comma-separated values, used for tabular data.
- **Excel:** Microsoft Excel files, used for storing and organizing processed data.
- **NetCDF4 (.nc):** Network Common Data Form, used for storing array-oriented scientific data.

3.2.2 Algorithm to convert transmission line data

In Figure 3.3, the process symbol "Convert transmission line data", refers to a Python script which processes transmission line data in SWEREF 99 TM coordinates, converts it to WGS 84 (longitude and latitude), and saves the processed data into a new JSON file. The purpose of the conversion is to create objects for the towers using their coordinates and to calculate the line segment lengths which will be used in the model later.

3.2.3 Algorithm to map the weather data to the tower coordinates

In Figure 3.3, the process symbol "Map weather data to towers", refers to a Python script which processes historical weather data from ERA5 for specific transmission line towers and saves the processed data into an Excel file.

First a function reads a JSON file containing transmission line data and extracts the coordinates of the towers for the specified line name. It returns a dictionary where each key is a tower name and the value is a list of its x and y coordinates. Then another function maps weather data from the ERA5 netCDF4 file to the coordinates of the towers. It creates a dictionary where each key is a tower name and the value is the interpolated weather data for the specified weather type. The function uses the latitude and longitude from the netCDF4 file to find the nearest weather data point for each tower and extracts the corresponding weather data. Finally, another function generates an Excel file containing the tower weather data for the specified weather types.

Table 3.4: Example table describing the output file of the weather data processing script. Each weather parameter is presented in a separate sheet.

Time	LineA.TA	LineA.TB	LineA.TC	LineA.TD
2012-01-01 00:00:00	0.123	0.456	0.789	0.101
2012-01-01 01:00:00	0.234	0.567	0.890	0.212
2012-01-01 02:00:00	0.345	0.678	0.901	0.323
2012-01-01 03:00:00	0.456	0.789	1.012	0.434
...
2022-01-01 23:00:00	1.234	1.567	1.890	1.101
2022-01-02 00:00:00	1.345	1.678	2.001	1.212

3.3 Probabilistic model & parameters

In this section, the probabilistic model is presented along with the mathematical theory. First, the main steps of the model are presented in an overview. Subsequently, the steps of the model are described in more detail.

3.3.1 Main steps of model algorithm

An overview of the main parts of the model can be seen in Figure 3.4. The model used in this thesis is based on demo code in Python provided by Statnett,

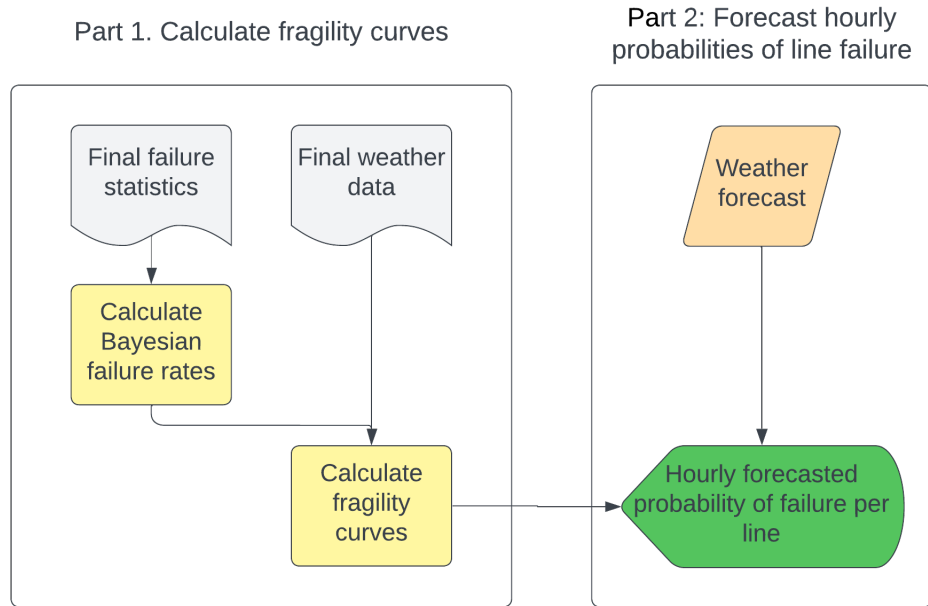


Figure 3.4: Flowchart of the main parts of the model.

as described in [10]. In the demo code, only wind was included as a weather factor. Lightning is included as a weather factor in Statnett's operational model; however, it was not included in the demo. Lightning has been added as described in [9] and also using parts of code provided from a test of the demo by the Hungarian TSO MAVIR, shared via ENTSO-E. The default failure rates in the demo code have been replaced with prior failure rates calculated in Excel based on Svk's disturbance database. The main outputs of the model are the fragility curves, which are curves describing the correlation between weather exposure and probability of failure for each transmission line. An overview of the part computing fragility curves is seen in Algorithm 1, referring to extracts of code found in the appendix.

3.3.2 Bayesian failure rates

The first step of the method is using a Bayesian updating scheme to calculate annual failure rates for each transmission line. This is done by using the general failure rate for all transmission lines in a category, and then adjusting the failure rate for each line based on the observed failures for each line in the category. In other words a prior estimate of the failure rate is created and then

Algorithm 1 VAFFEL Algorithm Main Steps Part 1: Fragility curves

Step 1: Model Preparations

1. Import necessary libraries and modules
2. Define essential classes and variables used in the model
3. Specify the overhead transmission lines under study
4. Load data related to historical failures of the lines

Step 2: Calculate Bayesian Failure Rates

1. Load prior failure rates from a specified file
2. Adjust the prior failure rates based on the length of transmission lines
3. Compute the posterior failure rates for the lines

Step 3: Construct Fragility Curves

1. Load relevant weather data for analysis
2. Load data for transmission lines after conversion
3. Store coordinates and segment lengths in a dictionary
4. Define functions to calculate wind and lightning exposure
5. Define an error function for optimization
6. Calculate probabilities of failure due to wind and lightning
7. Make an initial guess for shape parameters μ and σ
8. Define function to calculate μ and σ for fragility curves
9. Calculate fragilities and hourly probabilities for all lines, failure types, and sources

Step 4: Plot Results

1. Generate plots for hourly probabilities, fragility curves, and other relevant visualizations
-

updated to a posterior estimate using observations [10].

The motivation behind this is that some components are more prone to failure than others, even in the same weather conditions, causing more failures over time. By using the Bayesian updating scheme, both overall failure rates and individual differences are taken into consideration. In the best of worlds, the priors would be based on expert knowledge of individual failure rates due to factors such as year and method of construction, maintenance and terrain [10]. In this work, the prior failure rates are divided based on failure type, failure source and adjusted for length.

3.3.2.1 Bayes' Theorem

Bayes' Theorem is a fundamental concept in probability theory and statistics, providing a way to update the probability of a hypothesis as more evidence or information becomes available. It is a tool for making inferences and decisions under uncertainty [22].

Mathematically, Bayes' Theorem is expressed as:

$$P(H|E) = \frac{P(E|H) \cdot P(H)}{P(E)}$$

where:

- $P(H|E)$ is the posterior probability, the probability of the hypothesis H given the evidence E .
- $P(E|H)$ is the likelihood, the probability of the evidence E given that the hypothesis H is true.
- $P(H)$ is the prior probability, the initial probability of the hypothesis H before seeing the evidence E .
- $P(E)$ is the marginal likelihood or evidence, the total probability of the evidence E under all possible hypotheses [22].

In the context of this project, Bayes' Theorem is used to calculate posterior failure rates for transmission lines. By combining prior failure rates with observed data, the estimates are refined and more reliable failure rates, adjusted for the length of the transmission lines and other relevant factors are obtained.

3.3.2.2 Calculation of prior failure rates

The failure statistics is divided into categories based on failure source and failure type. The voltage levels chosen within this test are 220kV and 400kV, which are not divided in different categories. The prior failure rate is then adjusted to be expressed in number of failures per 100km of line in the category per year. For the 4 possible combinations of failure source and failure type, this results in 4 different prior failure rates. The lines can as earlier mentioned be further divided into categories based on factors such as age or maintenance schedule, but will not be further divided in this work. The prior failure rate for a category K is calculated using the following equation in this work:

$$\lambda_{\text{prior},K} = \frac{N_K}{L \cdot T} \quad (3.3)$$

where:

$\lambda_{\text{prior},K}$ = Prior failure rate for category K

N_K = Number of failures in category K

L = Total length of lines in kilometers (divided by 100 to convert to 100 km units)

T = Time period in years

3.3.2.3 Bayesian updating scheme in model

After calculating the prior failure rates, a Bayesian updating scheme based on Bayes Theorem is used to compute posterior failure rates, by adjusting the prior failure rate according to observed failures for the individual line. If the individual line in the category has many observed failures, the posterior failure rate will be increased, expressing that the individual line is more prone to failure than other lines in the same category. The opposite will happen if the individual line has few or no failures.

Mathematically, the annual failure rates are assumed to behave as a Poisson process. This means that failures will occur randomly according to a Poisson distribution, where the general annual failure rate is the mean rate, and all failures occur independently of each other [9] [10] [11].

The density function will then be described by $f_Y(y|\lambda)$, where λ is the annual failure rate for a transmission line i within category K and the random variable Y is the number of failures y_i^K per year [9] [10] [11].

$$f_Y(y|\lambda) = \frac{e^{-\lambda} \lambda^y}{y!} \quad (3.4)$$

Algorithm 2 Update Failure Rates

```

for each line  $l$  in  $study\_lines$  do
    {Iterate through all study lines} for each  $(ft, fs)$  in
     $it.product(failure\_types, failure\_sources)$  do {Iterate through all
    combinations of failure types and sources}
         $filtered\_df \leftarrow hist\_failures\_df[(hist\_failures\_df.Component ==$ 
         $l.long\_name) \& (hist\_failures\_df.Type ==$ 
         $ft) \& (hist\_failures\_df.Source == fs.lower())]$  {Filter historical
        failures}
         $number\_of\_faults \leftarrow len(filtered\_df)$  {Count the number of
        faults}
         $lambda\_prior \leftarrow failure\_rates[(l, ft, fs)].lambda\_prior$  {Re-
        trive prior failure rate}
         $alpha\_posterior \leftarrow 1.0 + number\_of\_faults$  {Calculate posterior
        alpha}
         $beta\_posterior \leftarrow 1.0 / lambda\_prior + number\_of\_years$  {Calcu-
        late posterior beta}
         $lambda\_posterior \leftarrow round(alpha\_posterior / beta\_posterior, 4)$ 
        {Compute posterior failure rate}
         $failure\_rates[(l, ft, fs)].lambda\_posterior \leftarrow$ 
         $round(lambda\_posterior, 4)$  {Update failure rate with posterior
        value}
    end for
end for

```

If there are y_1, y_2, \dots, y_n observed failures for category K for each year over a period of n years, the likelihood function becomes [9] [10] [11]:

$$p(y|\lambda) = \prod_{i=1}^n \frac{\lambda^{y_i} e^{-\lambda}}{y_i!} \quad (3.5)$$

$$\propto \lambda^{\sum y_i} e^{-n\lambda} \quad (3.6)$$

Using Bayes theorem, the general failure rate is modeled as the prior with a gamma distribution given by [9] [10] [11]

$$p(\lambda) = \frac{\beta^\alpha \lambda^{\alpha-1} e^{-\lambda\beta}}{\Gamma(\alpha)} \quad (3.7)$$

where $\Gamma(\alpha)$ is the Gamma function and α and β are the parameters of the Gamma distribution. The expected value of a Gamma-distributed variable X is given by [9] [10] [11]

$$E[X] = \frac{\alpha}{\beta} \quad (3.8)$$

Since the gamma distribution is the conjugate prior for the Poisson process [23], the posterior distribution is also gamma distributed, but with new parameters α' and β' such that [9] [10] [11]

$$\alpha' = \alpha + \sum_i y_i \quad (3.9)$$

$$\beta' = \beta + n \quad (3.10)$$

This results in the Bayesian adjusted posterior failure rate λ_B is given by

$$\lambda_B = \frac{\alpha'}{\beta'} = \frac{\alpha + \sum_i y_i}{\beta + n} \quad (3.11)$$

which is the actual calculation done by the program, as seen in pseudocode 2. The specific model assumes an exponential distribution for the failure rate, which is why $\alpha = 1$ and $\beta = \frac{1}{\lambda}$ [9] [10] [11].

3.3.3 Weather exposure

In the Vaffel-tool wind speed and lightning are the weather factors included. Wind exposure is handled by first defining a minimum threshold of wind speed w_{thresh} above which failures can be classified as related to wind. The energy

of the wind is proportional to the cube of wind speed, motivating the modeling of wind exposure as the cube of wind speed w_i^t above the threshold at the time t for line segment i [11] [10] [11].

$$\hat{w}_{i,t}^{wind} = \begin{cases} \alpha_w l_i (w_{t,i} - w_{\text{thresh}})^3, & w_{t,i} \geq w_{\text{thresh}}, \\ 0, & w_{t,i} < w_{\text{thresh}}. \end{cases} \quad (3.12)$$

α_w is a scale factor used to normalize the input to the fragility curve for wind speed [11] [10].

The lightning exposure for line segment i at time t is defined as follows [9]

$$w_{lightning}^{i,t} = \alpha_K \max(0, K_i^t - K_{\text{thresh}})^2 + \alpha_{TT} \max(0, TT_i^t - TT_{\text{thresh}})^2 \quad (3.13)$$

where K_i^t and TT_i^t are the values of the K and TT indices at time t for segment i , K_{thresh} and TT_{thresh} are threshold values below which the index does not contribute to the failure probability, and α_K and α_{TT} are scale parameters. In this work $\alpha_K = 0.88$ and $\alpha_{TT} = 0.12$ as in [9] to reflect seasonal difference weights.

3.3.4 Fragility curves

The fragility curves are in a way the basis of the method, or the actual product used for prediction of failure with weather prognosis later on. The fragility curves establish the correlation between the weather exposure of a transmission line and its probability of failure. A cumulative lognormal distribution is used to model the relation using the following lognormal density function [9] [10]

$$f(x; \mu_l, \sigma_l) = \frac{1}{x\sigma_l\sqrt{2\pi}} \exp\left(-\frac{(\ln(x) - \ln(\mu_l))^2}{2\sigma_l^2}\right) \quad (3.14)$$

where μ_l is a scale parameter and σ_l is a shape parameter shaping the curve of the cumulative lognormal distribution.

Then the probability of failure for line segment i of line l at time t with weather exposure \hat{w} is [9] [10]

$$p_{i,l}^t = F(\hat{w}; \mu_l, \sigma_l) = \int_0^{\hat{w}} f(\xi; \mu_l, \sigma_l) d\xi \quad (3.15)$$

giving the total probability of failure for the line at time t

$$p_{tl} = 1 - \prod_{i=1}^N (1 - p_{ti,l}) \quad (3.16)$$

[9] [10] where $p_{i,l}^t$ is the probability of failure of line segment i at time t and N is the number of segments. The assumption is that the fragility is the same for all line segments, only differing due to weather exposure. The parameters μ_l and σ_l of the fragility curve are found in an optimization process [9] [10]. First, an historical hourly time series of weather exposure based on the reanalysis data is calculated for each line. In the weather exposure calculation a simplification is done which entails choosing the line segment with the maximum value of respective weather factor and using it as the weather exposure for the whole line. Every time step is seen as a Bernoulli experiment with failure probability equal to the fragility value, allowing to determine the values of μ_l and σ_l by setting the mean yearly number of failures equal to the Bayesian failure rate λ_B

$$\lambda_B = \frac{1}{k} \sum_t p_l^t \quad (3.17)$$

where k is the number of years of reanalysis and p_l^t is found by optimizing the minimized squared difference between the terms according to a penalty function g below, which is done using the L-BFGS-B-method in Python.

Let the penalty function g be defined as [9] [10] [11]

$$g(p_l^t; \mu, \sigma) = \left(\lambda_B - \frac{1}{k} \sum_{t=0}^T p_l^t \right)^2 \quad (3.18)$$

Then, μ_l and σ_l are found by minimizing the equation [9] [10] [11]:

$$\mu_L, \sigma_L = \arg \min_{\mu, \sigma} g(p_L^t; \mu, \sigma). \quad (3.19)$$

The process is summarized in an overview flowchart in Figure 3.5.

3.3.5 Forecast of line failure probabilities

The second part of the model has the purpose of forecasting hourly failure probabilities for each overhead line using the fragility curves from part 1 of the model together with a medium range hourly weather forecast for each weather parameter. The basic concept is to exploit the calculated correlation

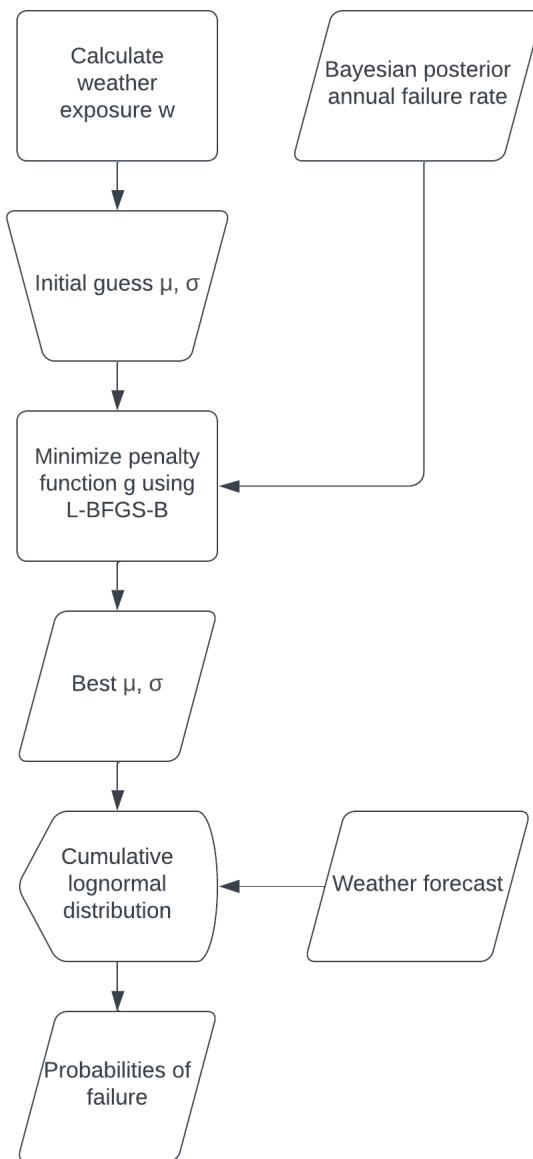


Figure 3.5: Overview of the process of computing fragility curves.

between the weather exposure and probability of failure, resulting in a specific probability given for each value of weather exposure. A specific probability will be given for temporary and permanent failures respectively for each weather factor [9] [10] [11].

In this work the forecast function is demonstrated using historical weather data as input in order to simplify. In real use of the model, actual forecasted data for each parameter should be used.

3.4 Reliability and validity assessment

In order to assess the validity of the method used with Svk data, the calculated hourly probabilities are analysed in different steps. The first step is to reanalyse historical failures visually by loading the weather data for the time period of the actual failure into the forecasting part of the model and comparing the predicted probability of failure with each outcome of actual failure to analyse correlation. The second step is to quantify the validity of the model using the Brier Score originally described in paper [24]. The Brier Score is used in a penalty term in the model by Statnett, which is however not implemented in this thesis work [10].

The Brier score is a metric used to measure the accuracy of probabilistic predictions. It enables a comparison of the accuracy over time as the model is updated with more data and also when tuning parameters. It is calculated as the mean squared difference between the predicted probability of an event occurring and the actual outcome. The formula for the Brier score is given by [24]:

$$\text{Brier Score} = \frac{1}{N} \sum_{i=1}^N (f_i - o_i)^2 \quad (3.20)$$

where:

- N is the number of predictions,
- f_i is the predicted probability of the event occurring,
- o_i is the actual outcome (1 if the event occurred, 0 if it did not).

The Brier score ranges from 0 to 1, where a score of 0 indicates perfect accuracy, and a score of 1 indicates the worst possible accuracy. Lower Brier scores indicate better predictive accuracy. The calculation is done in python

where an array of hourly predictions of failure for the chosen line and time period are compared to the actual outcome in the failure statistics [24].

Chapter 4

Results and Analysis

In this chapter the results of the modelling are presented and discussed. First the Bayesian failure rates are presented, then the fragility curves for both single segments and full lines, followed by the hourly probabilities of failure for a selected time period and an analysis of past actual failures demonstrating the predictive capabilities of the model. Finally the reliability and validity of the model is assessed.

4.1 Bayesian failure rates

The Bayesian failure rates are calculated for all three lines where the priors are based on the full failure statistics for all lines and the posteriors are calculated according to the Bayesian Updating Scheme described in the method. The results are seen in Table 4.1, where the adjustments of the failure rates based on the number of observed failures is demonstrated. The lines have a failure rate calculated separately for each combination of failure source and failure type. As anticipated the posterior failure rate shows an increase from the prior failure rate in cases where many failures were observed.

Table 4.1: Prior and posterior failure rates for Line A,B and C based on failure statistics for 1998-2023. The priors are adjusted to the line lengths, which is why the priors are different between the lines, as they are of different lengths.

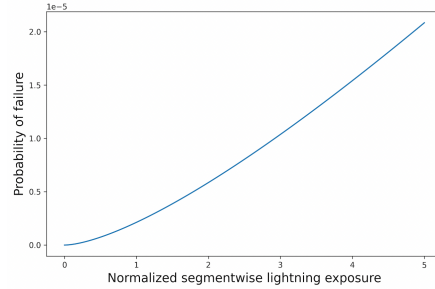
Line	Failure Type	Failure Source	Prior	# of Failures	Posterior
Line A	Permanent	Wind	0.0017	0	0.0016
Line A	Permanent	Lightning	0.0017	0	0.0016
Line A	Temporary	Wind	0.0133	1	0.0198
Line A	Temporary	Lightning	0.2429	30	1.0293
Line B	Permanent	Wind	0.0005	0	0.0005
Line B	Permanent	Lightning	0.0005	0	0.0005
Line B	Temporary	Wind	0.0039	13	0.0496
Line B	Temporary	Lightning	0.0712	4	0.1249
Line C	Permanent	Wind	0.0011	0	0.0011
Line C	Permanent	Lightning	0.0011	0	0.0011
Line C	Temporary	Wind	0.0082	0	0.0068
Line C	Temporary	Lightning	0.1499	0	0.0306

4.2 Fragility curves

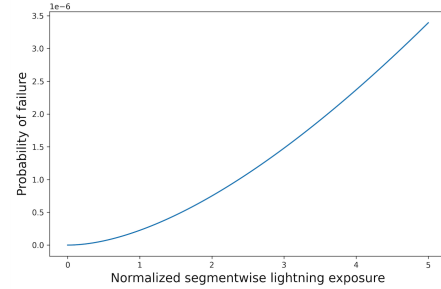
4.2.1 Single segment fragility curves

Figure 4.1a and 4.1b show the single segment fragility curves for lightning for Line A and B and Figures 4.2a and 4.2b show the single segment fragility curves for wind for Line B and C. The x-axis show the normalized segmentwise weather exposure, which is based on the calculations for each respective weather factor exposure, and the y-axis show the corresponding probability of failure, related to the specific exposure. The scales on the y-axes differ between the lines, which underlines the difference in how prone each line is to fail, given a certain weather exposure. As earlier explained, the method of creating fragility curves in this work assumes that each line and each line segment has an individual vulnerability, based on a combination of different factors such as age, maintenance schedule and environmental factor, which is expressed here in the fragility curves. In Figure 4.1 it can be seen that when Line A and Line B experience the same lightning exposure, Line A is almost 6 times more likely to fail than Line B. In Figure 4.2 we can see another factor influencing the fragilities, which is the line length, adjusted for in the calculation of Bayesian failure rates. In this method used, the vulnerability to failure will increase proportionally to line length, due to the assumption

that the probability of failure follows the amount of line that is exposed. This assumption can be investigated, as there might be other correlations between line length and probabilities of failure that are more accurate.

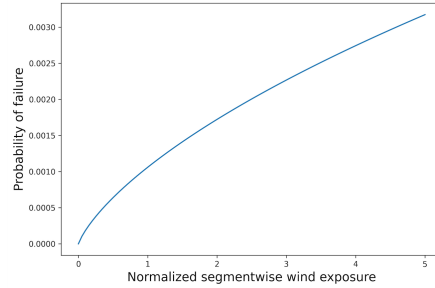


(a) Fragility curve for lightning for a single segment of Line A.

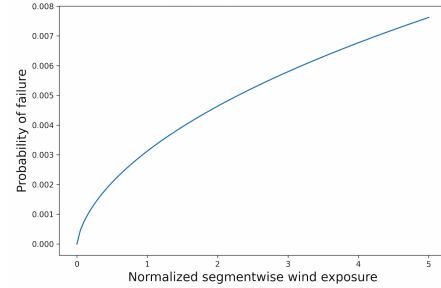


(b) Fragility curve for lightning for a single segment of Line B.

Figure 4.1: Comparison of fragility curves for lightning for different lines. Note that the scales on the y-axes are different due to different fragilities of the lines.



(a) Fragility curve for wind for a single segment of Line B.



(b) Fragility curve for wind for a single segment of Line C.

Figure 4.2: Comparison of fragility curves for wind for different lines. Note that the scales on the y-axes are different due to different fragilities of the lines.

4.2.2 Full line fragility curves

The full line fragility curves demonstrate the relation between weather exposure and probability of failure for each line and weather factor. The curves are constructed by using the time series of weather data and for each hour plotting the probability of failure for the line segment with the maximum

weather exposure. Lightning exposure is calculated for K-index and Total Totals-index together which affects visualisation of the thresholds.

Figure 4.3 and Figure 4.4 show the fragility curves for K-index and Total Totals-index for Line A, which is the line with most observed failures due to lightning. The curves have the expected shape with an increase in probability following an increase in exposure.

Fragility curves for wind are plotted for Line B in Figure 4.5 and for Line C in Figure 4.6 showing the difference in exposure and probability of failure between the lines, where Line B reaches both higher wind speeds and probabilities compared to Line C, which corresponds correctly to the number of observed failures which is higher for Line B.

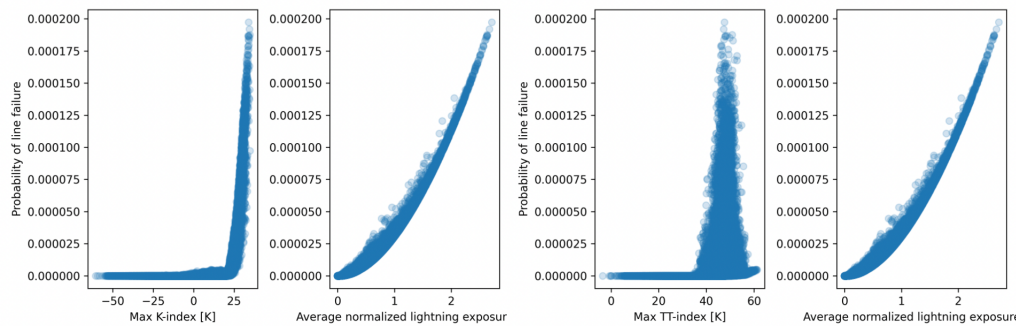


Figure 4.3: Fragility curve K-index for Line A.

Figure 4.4: Fragility curve Total Totals-index for Line A.

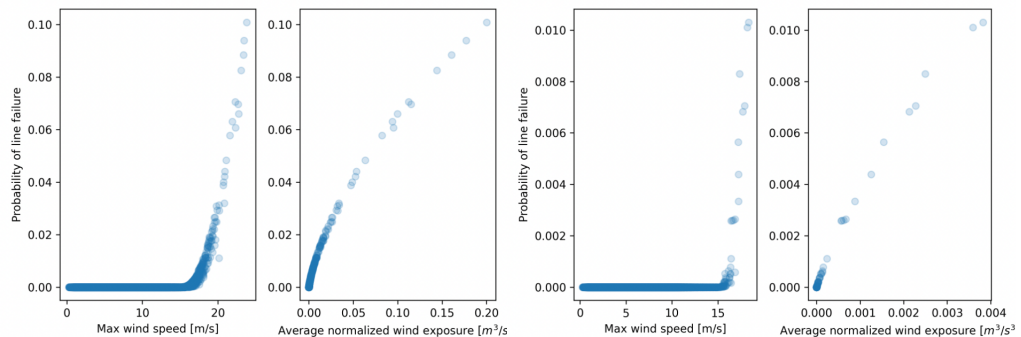


Figure 4.5: Fragility curve wind for Line B.

Figure 4.6: Fragility curve wind for Line C.

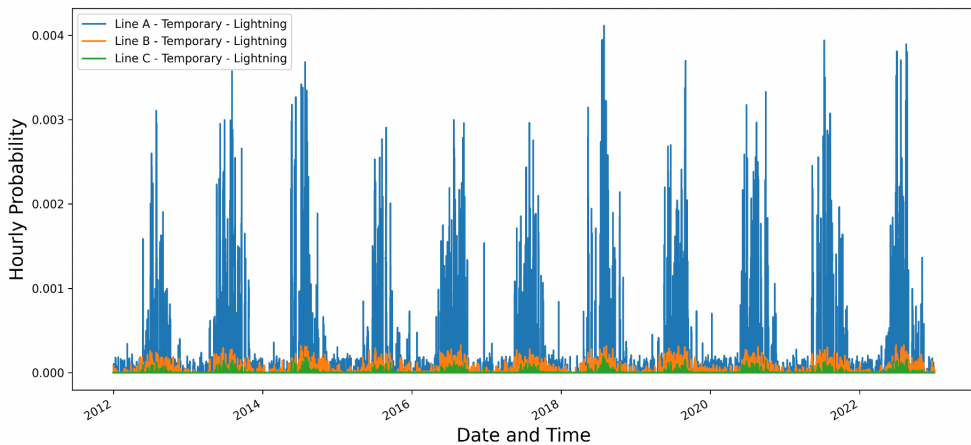


Figure 4.7: Hourly probabilities of failure due to lightning 2012-2022.

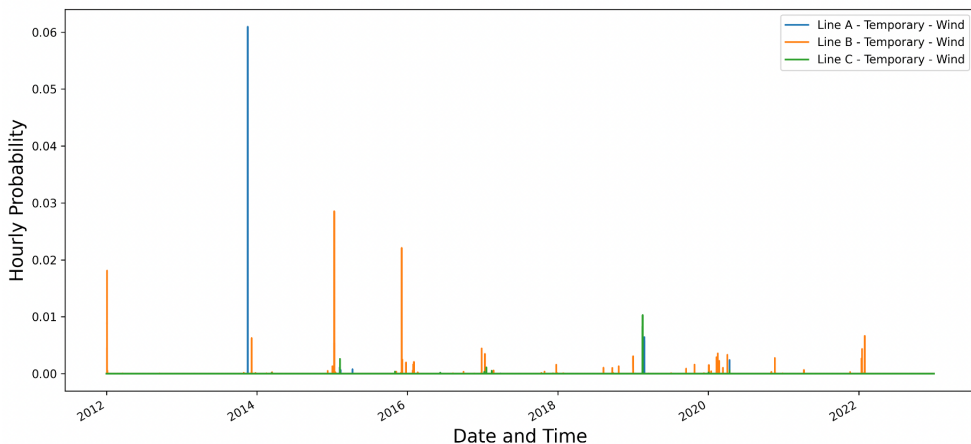


Figure 4.8: Hourly probabilities of failure due to wind 2012-2022.

4.3 Reliability and Validity Analysis

In this section the reliability and validity of the model and the results are tested and evaluated.

4.3.1 Hourly probabilities of failure

Figure 4.7 shows the hourly probabilities of failure due to lightning for the three overhead lines from year 2012 to 2022. The result shows that the probability of failure follows a seasonal variation, with a higher concentration of increased probabilities of failure during the summer months May to

September.

The resulting probabilities for the different overhead lines correspond with their individual calculated fragility. Line A was more prone to failure due to lightning with a total of 30 temporary faults due to lightning in the statistics and shows the largest increased probabilities of failure over the time period, whereas Line B and Line C with 4 and 0 faults due lightning respectively show lower probabilities of failure in the hourly time series.

Figure 4.8 shows the hourly probabilities of failure due to wind during the same time period. In general the occurrences of an increased probability are less frequent than for lightning, although the existent peaks in probability are higher.

4.3.2 Historical failures due to wind

In Figure 4.9 a time period including a series of actual failures due to wind for Line B is modelled. The result shows an increased probability of failure coinciding with the actual faults, indicating a correct calibration of the model. This indication however needs to be validated by further testing, as it could also be coincidental.

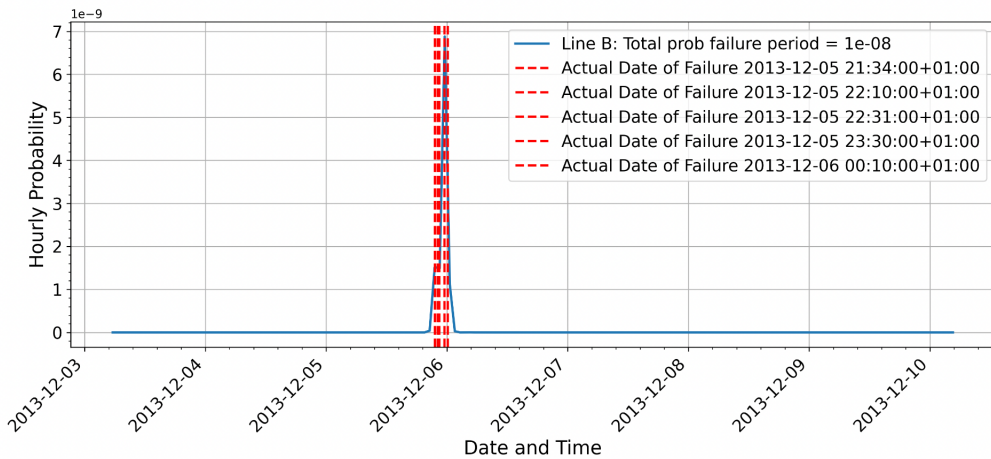


Figure 4.9: Analysis of historical failures due to wind Line B coinciding with increased probability of failure.

4.3.3 Historical failures due to lightning

Figure 4.10, 4.11, 4.12 shows three examples of time periods modelled where actual failures occurred due to lightning for Line A, where the calculated probability of failure accurately increased at the time of the failure. All three graphs have a fixed y-axis for comparison purposes. A majority of the analysed historical failures in this work have a similar correlation to increased probabilities, where some are more clearly correlated than others. Since the quantity of available failures to analyse for the given time period and chosen transmission lines is relatively low, it is difficult to draw solid conclusions about the models performance based on the output. An observation that however is valid is that the model can produce relevant output based on the currently available data.

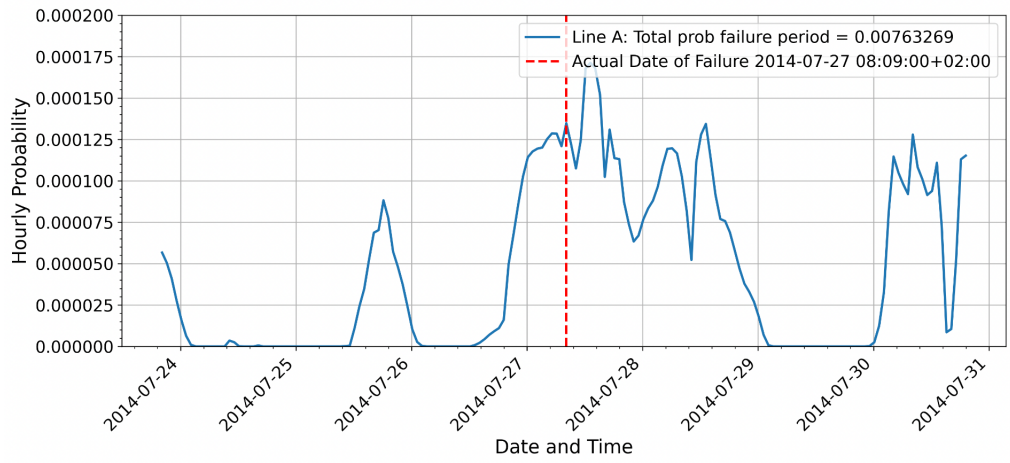


Figure 4.10: Analysis of historical failure due to lightning Line A coinciding with increased probability of failure.

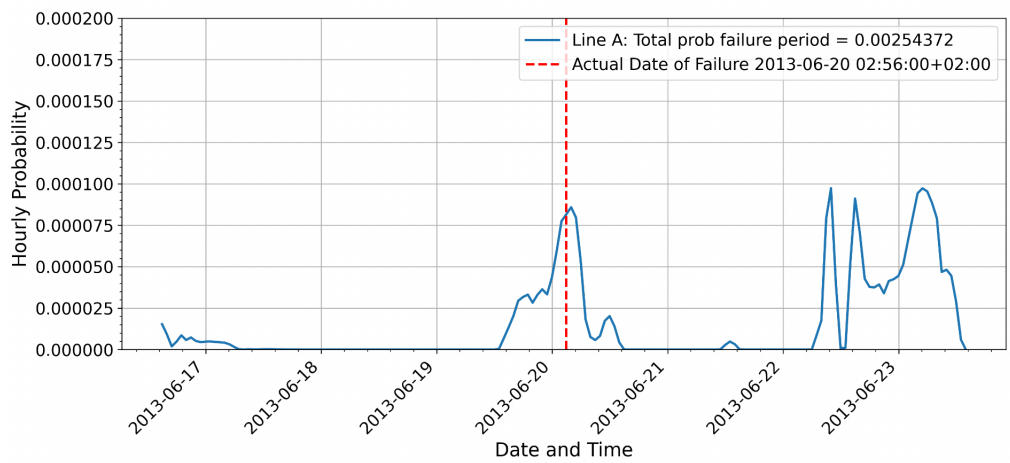


Figure 4.11: Analysis of historical failures due to lightning Line A coinciding with increased probability of failure.

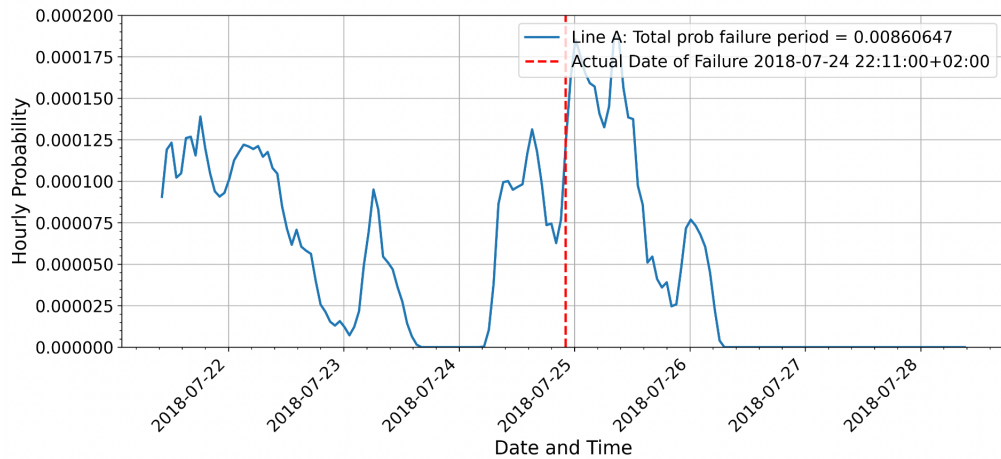


Figure 4.12: Analysis of historical failures due to lightning Line A coinciding with increased probability of failure.

4.3.4 Mismatches between failures and predictions

In the analysis of historical failures, a few examples of mismatches between the predicted probability and actual failures were found, as seen in Figure 4.13 for wind and Figure 4.14 for lightning. Possible explanations of this could be that the ERA5 weather data from Copernicus CDS has too low resolution leading to accuracy issues in the prediction. The weather data is based on a grid of $0.25^\circ \times 0.25^\circ$ in longitude and latitude which equals to 27,75 km x 27,75 km. This can be compared to the segment lengths, which is the entity the exposure is calculated for, of ca 330 metres. The result of this is a less exact estimation of the actual exposure per segment and line during the analysed time period.

Other explanations for the mismatch could include local variations in weather due to specific topography and environmental factors not accounted for in detail in the modeled weather data, causing a time shift in weather exposure, or other issues related to the inherent uncertainties stemming from the probabilistic nature of the model.

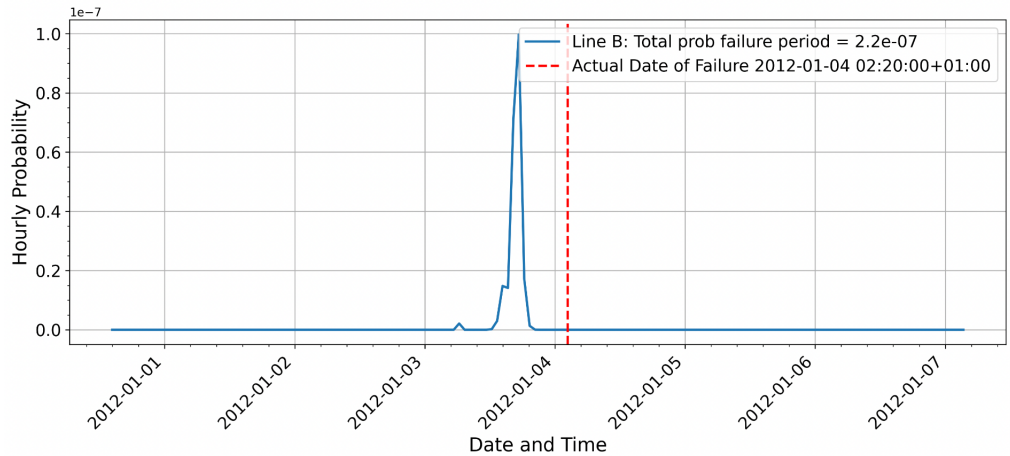


Figure 4.13: Analysis of historical failure wind Line B mismatched in time with increased probability of failure.

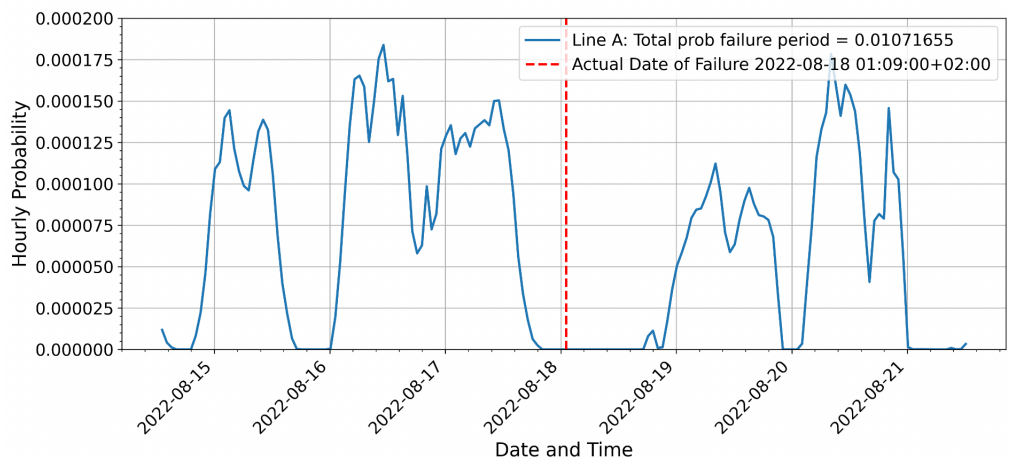


Figure 4.14: Analysis of historical failures due to lightning Line A mismatched in time with increased probability of failure.

4.3.5 Forecasted probabilities of failure

Another test performed was to load weather data for 2023 in the forecasting part of the model and analyse the predicted probability of failure during an actual failure which occurred. The difference of this test compared to the other analysed historical failures is that the weather data for 2023 was not used as input data for the fragility curves, which the forecast is based on. No major difference in accuracy is anticipated compared to the predictions using the same weather data as used in construction of the fragility curves.

The result can be seen in Figure 4.15, where the actual failure due to lightning at Line A coincides with a predicted increased probability of failure. For comparison purposes the same time period was modelled for Line B and Line C in Figure 4.16 and 4.17 where no failures were registered. The comparison shows increased probabilities of failure for both lines, of the same magnitude as for Line A. This illustrates the possibility of increased predicted failures without an actual failure occurring. One must remember that even though the probability of failure is increased, the most probable outcome in all of these resulting predictions is still no failure.

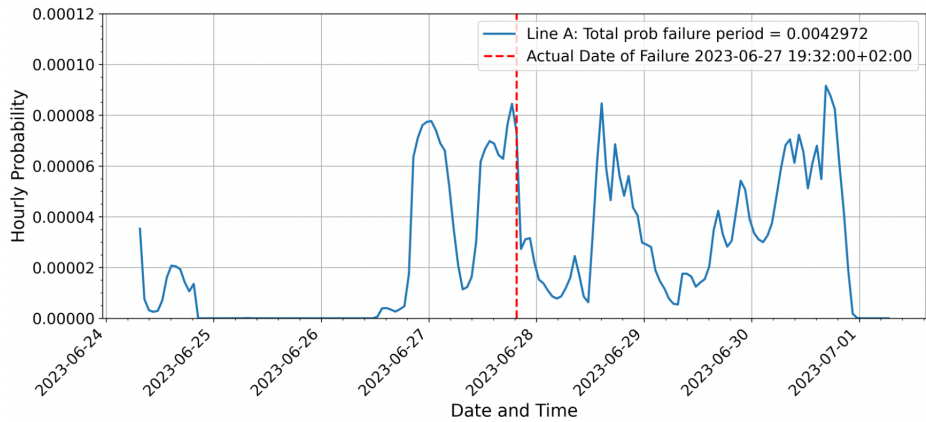


Figure 4.15: Forecasted probabilities of failure on new data for 2023 Line A.

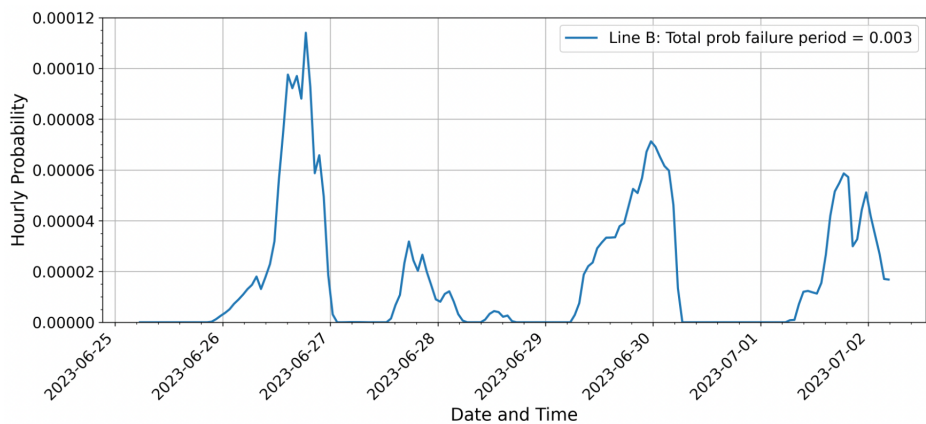


Figure 4.16: Forecasted probabilities of failure on new data for 2023 Line B without actual failure occurring.

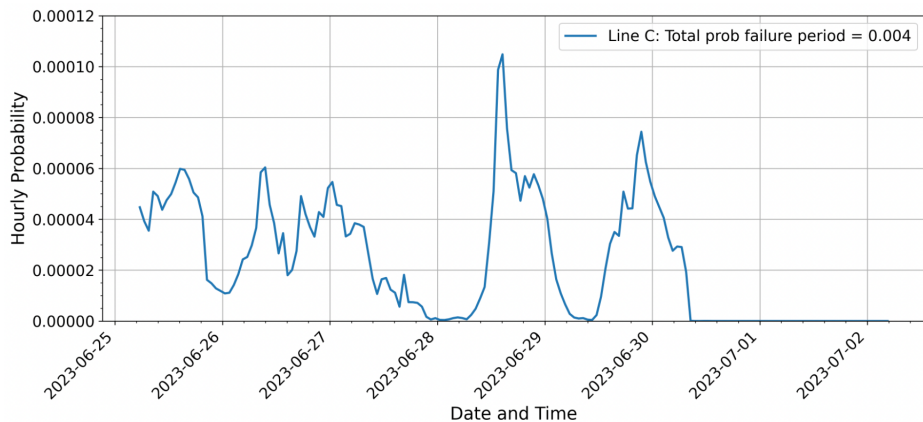


Figure 4.17: Forecasted probabilities of failure on new data for 2023 Line C without actual failure occurring.

4.3.6 Brier Score

In an attempt to validate the model quantitatively, the Brier Score is calculated for four different prediction approaches for each line respectively. The scores should be interpreted carefully, due to limitations in the Brier Score. The approaches are the modelled predictions of failure due to wind and lightning and also predictions using a constant failure rate equal to the prior failure rates used as inputs in the model.

In Figure 4.18 the result is shown on a logarithmic scale. The logarithmic scale is motivated by the large difference between the prediction accuracy of the lightning model compared to the wind model. The scores indicate that both prediction models perform better than if applying a constant failure rate, which is anticipated. A constant failure rate means that the predicted probability of failure is constant for every hour during the year. Had the model predicted worse than the constant failure, there would be a strong indication that the model was not accurate and not producing useful information. The opposite result, which is the case, indicates that the model is relevant and produces useful information.

Another indication is that the wind model has higher accuracy than the lightning model. The first consideration when interpreting this result is that it could be affected by the limited amount of data, especially for failures due to wind. If however the result consist in trials with expanded data coverage, the difference in accuracy could be explained by the difficulty of determining where a specific lightning will strike within a thunderstorm adding a random factor in the exposure, whereas wind exposure is more evenly distributed.

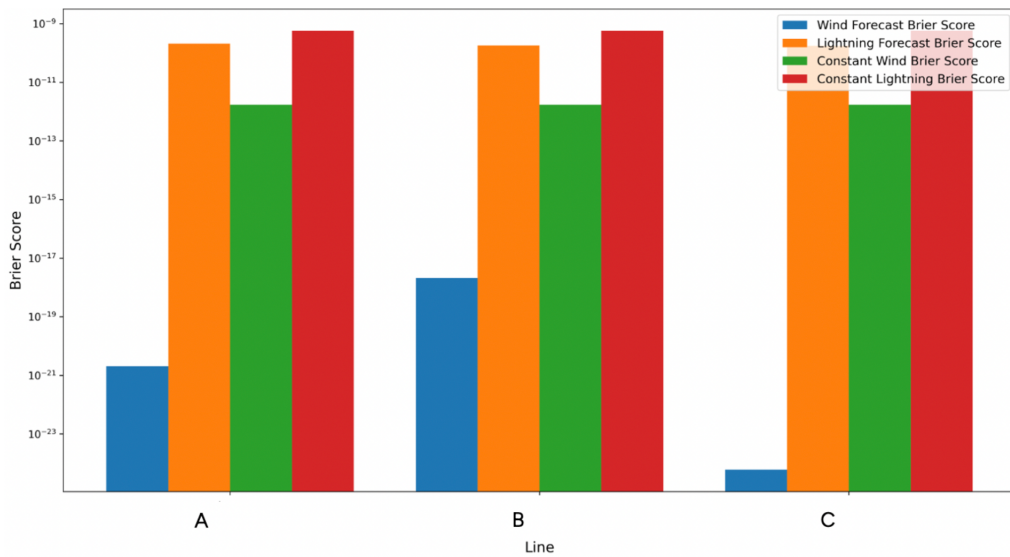


Figure 4.18: Comparison of Brier Scores for all three lines including constant failure rate, wind and lightning modelling.

Another explanation could lie in calibration of the model, where different factors in the calculation could be more accurate for wind than lightning. A third explanation which is tied to the Brier Score itself, is that there is a larger number of zero-elements in the arrays of predicted probabilities and actual outcomes for wind than for lightning, which reduces the score for the wind model.

Chapter 5

Discussion

Although the results from the modelling overall indicate that the method is useful for implementation of PRA in the short term operational planning, the validation of the model is not completed within the scope of this work. The main reason for this is the limited basis of data in terms of number of lines, years of weather data and years of failure statistics. The most important next step in the validation is to include more transmission lines for testing, to be able to draw conclusions based on statistically significant results. An increased basis of data also enables different types of validation from analysis on an aggregated level.

The results of this work can however support that the method is relevant, and that Svk has a sufficient amount of data today to get meaningful results from the model.

Areas of improvement of the input data are higher resolution of weather data and higher percentage of given failure source in the failure statistics. Possible improvement for the model as used within this work is including the Brier Score as a penalty term in the construction of the fragility curves as described in [10]. This was not included in this version of the model as a simplification. The calculations of the priors can also be improved by for example dividing the categories differently based on information about environmental factors, age and maintenance schedules. When changing the priors it is important to observe and analyse the effect on the accuracy of predictions. The model in the current form showed sensitivity of the accuracy when changing the priors, which might however be alleviated with inclusion of the penalty term mentioned above.

Regarding the larger question of how to implement PRA in the short term operational planning, it is important to remember that there are several other

components in the transmission grid with failures and several other factors causing these failures. The method in this work can however act as a base upon which extensions to other areas can be added.

With the increased use and popularity of artificial intelligence, models utilizing various types of machine learning and neural networks are emerging for forecasting. These advanced models can analyze vast amounts of data and identify patterns that might be missed by traditional methods. However, an important aspect to consider when using 'black box' models for forecasting is the liability and responsibility associated with the decisions based on them. Since the internal workings of these models are often not transparent or easily understandable, it becomes challenging to explain their predictions and ensure accountability. This opacity raises concerns about trust, ethics, and the potential consequences of relying on AI-driven decisions, which should be considered in a critical field as the operation of transmission grid.

In contrast, simpler models such as this one offer greater transparency and interpretability. They allow stakeholders to easily understand how predictions are made, fostering trust and enabling straightforward accountability. While they may not always match the predictive power of advanced AI models, the balance between accuracy and interpretability must be carefully weighed, especially in critical applications where the consequences of decisions are significant. Therefore, when implementing forecasting models, it is essential to evaluate the trade-offs between the sophistication of the model and the ability to clearly justify its outputs.

Chapter 6

Conclusions and Future work

In this chapter the conclusions and limitations are presented, together with reflections and suggestions for future work.

6.1 Conclusions

The overall purpose of the project was to investigate how Svk can implement PRA in short term operational planning based on the VAFFEL-method and if there is sufficient data available today to start implementation divided into five subgoals including to identify how the VAFFEL-method can be incorporated in existing internal operational processes, to identify the data required for using the method and whether Svk has a sufficient data availability today to produce relevant results with the method, to identify how the existing data collection can be improved in terms of quality and quantity, to produce more accurate results. Test the model with Svk data and identify how the VAFFEL-method can be extended or adjusted to bring maximum value at Svk, in accordance with the requirements by ACER in CSAM.

The conclusions are that the VAFFEL method is feasible to implement in short-term operational planning and that Svk has sufficient quantity and quality of data available for the model to produce relevant results. The probabilities generated by the model could be incorporated into the current contingency analysis in operational planning, after further validation with a larger data set. Data collection can be improved by increasing the percentage of faults reported with a known failure source and gathering weather data with higher resolution, which would enhance the model's accuracy. Currently, the model indicates better accuracy for predicting probabilities of failure due to wind than lightning; however, it still performs better for both failure sources

compared to a constant failure rate. These conclusions need to be validated with further testing, since the data set in this work is limited.

6.2 Limitations

Regarding both the model and the results, there are limitations that must be considered when interpreting the conclusions. Concerning the model, aside from the predefined delimitations in the chosen weather factors and components, there are inherent simplifications and limitations. For example, the categorization of overhead lines is coarse; it does not account for variables such as age, maintenance schedules, or local environmental factors.

Regarding the input data, the TT-index and K-index are sensitive to local variations, and seasonal variation in these indices has not been accounted for. As mentioned earlier the resolution of the weather data in this project is rather low, and a higher resolution would be beneficial for the accuracy of the model [21].

The results are primarily limited by the narrow scope tested in the project, which restricts the ability to draw statistically significant conclusions. Only three overhead lines were included, and the weather data used spans only 12 years. This, combined with the infrequent occurrence of overhead line failures over a transmission line's lifespan, makes the model sensitive to minor changes.

6.3 Future work

In this section suggestions for future work on the theme are presented.

6.3.1 Set up the forecasting part

The next step in this work is to establish the actual forecasting component of this model to test it with real forecasts. To achieve this, forecasted weather data must be collected in the appropriate format for all relevant weather factors. If the K-index and Total Totals-index are not directly available, they can be calculated using the inputs in equations 3.1 and 3.2.

6.3.2 Validation of the model on an aggregated scale

This thesis project does not attempt to validate the model on an aggregated scale, which remains for future work. The first step would be to include all

transmission lines, load weather data for a longer time span and construct fragility curves. Thereafter different analyses can be made on an aggregated results to confirm the accuracy of the model.

6.3.3 Including more components and factors

An obvious direction for future work in the implementation of PRA in short-term operational planning is to calculate probabilities for additional components beyond just overhead lines, such as transformers, cables, and circuit breakers. To achieve accurate forecasts of such probabilities, research must be conducted to identify which exogenous factors correlate with the failure rates of different components. As evidenced by the differences observed between lightning and wind predictions, various factors can present unique challenges.

6.3.4 In depth comparison to other forecasting models

This thesis project has not included an in depth-comparison to other forecasting models. This could be performed for a chosen set of models which can be compared using a common evaluation framework.

References

- [1] ENTSO-E, “Biennial progress report on operational probabilistic coordinated security assessment and risk management,” 2023. [Pages 1, 2, 5, 7, and 8.]
- [2] “Acer decision on csam: Annex i methodology for coordinating operational security analysis in accordance with article 75 of commission regulation (eu) 2017/1485 of 2 august 2017 establishing a guideline on electricity transmission system operation,” Online, June 2019, decision by the Agency for the Cooperation of Energy Regulators (ACER). [Pages 1, 6, and 7.]
- [3] “Generally accepted reliability principle with uncertainty modelling and through probabilistic risk assessment | garpur project | fact sheet | fp7.” [Online]. Available: <https://cordis.europa.eu/project/id/608540> [Pages 5 and 6.]
- [4] J. McCalley, S. Asgarpoor, L. Bertling Tjernberg, R. Billinton, H. Chao, J. Chen, J. Endrenyi, R. Fletcher, A. Ford, C. Grigg, G. Hamoud, D. Logan, A. Meliopoulos, M. Ni, N. Rau, L. Salvadori, M. Schilling, Y. Schlumberger, A. Schneider, and R. Billinton, “Probabilistic security assessment for power system operations,” vol. 1, 07 2004. doi: 10.1109/PES.2004.1372788. ISBN 0-7803-8465-2 pp. 212 – 220 Vol.1. [Page 6.]
- [5] Agency for the Cooperation of Energy Regulators, “The agency: About acer.” [Online]. Available: <https://www.acer.europa.eu/the-agency/about-acer> [Page 6.]
- [6] European Commission, “Commission regulation (eu) 2017/1485 of 2 august 2017 establishing a guideline on electricity transmission system operation,” 2017. [Online]. Available: <https://eur-lex.europa.eu/legal-content/EN/TXT/?uri=CELEX:32017R1485> [Page 6.]

- [7] Svenska Kraftnät, “Uppdrag att lämna förslag till norm för driftsäkerhet i fredstida normalläge,” Svenska Kraftnät, Delrapportering 2, Apr. 2024, Ärende nr: Svk 2023/2188. [Online]. Available: <https://www.svk.se/siteassets/om-oss/rapporter/2024/uppdrag-att-lamna-for-slag-till-norm-for-driftsakerhet-i-fredstida-normallage.pdf> [Page 8.]
- [8] ENTSO-E, “2022 nordic and baltic grid disturbance statistics,” 2023. [Pages xi, 8, 9, and 10.]
- [9] . R. Solheim and T. Trötscher, “Modelling transmission line failures due to lightning using reanalysis data and a bayesian updating scheme,” in *2018 IEEE International Conference on Probabilistic Methods Applied to Power Systems (PMAFS)*, 2018. doi: 10.1109/PMAFS.2018.8440365 pp. 1–5. [Pages 10, 21, 24, 26, 27, 28, and 30.]
- [10] . R. Solheim, T. Trötscher, and G. Kjølle, “Wind dependent failure rates for overhead transmission lines using reanalysis data and a bayesian updating scheme,” in *2016 International Conference on Probabilistic Methods Applied to Power Systems (PMAFS)*, 2016. doi: 10.1109/PMAFS.2016.7764104 pp. 1–7. [Pages 10, 15, 21, 23, 24, 26, 27, 28, 30, and 47.]
- [11] . R. Solheim, I. Ligaarden, B. A. Høverstad, T. Trötscher, M. Andersen, and M. Korpas, “Vaffel - a tool for forecasting transmission line failures based on bayesian updating, reanalysis data and medium range weather forecasts,” in *Proceedings of the PMAFS 2024 Conference*, Oslo, Norway, 2024, accepted for publication. [Pages 10, 24, 26, 27, 28, and 30.]
- [12] J. Björns, “Transmission expansion planning considering probabilistic risk assessment implemented at swedish national grid,” Master’s thesis, Stockholm, Sweden, 2023. [Online]. Available: <https://www.svk.se/siteassets/5.jobba-har/dokument-exjobb/transmission-expansion-planning-considering-probabilistic-risk-assessment.pdf> [Page 10.]
- [13] Z. Yun, Q. Zhou, Y. Feng, D. Sun, J. Sun, and D. Yang, “On-line static voltage security risk assessment based on markov chain model and svm for wind integrated power system,” in *2017 13th International Conference on Natural Computation, Fuzzy Systems and Knowledge Discovery (ICNC-FSKD)*, 2017. doi: 10.1109/FSKD.2017.8393162 pp. 2469–2473. [Pages 10 and 11.]

- [14] W. O. Taylor, S. Nyame, W. Hughes, M. Koukoula, F. Yang, D. Cerrai, and E. N. Anagnostou, “Machine learning evaluation of storm-related transmission outage factors and risk,” *Sustainable Energy, Grids and Networks*, vol. 34, p. 101016, 2023. doi: 10.1016/j.segan.2023.101016. [Online]. Available: <https://www.sciencedirect.com/science/article/pii/S2352467723000243> [Pages 10 and 11.]
- [15] Y. Zhu and C. Singh, “End-to-end topology-aware machine learning for power system reliability assessment,” in *2022 17th International Conference on Probabilistic Methods Applied to Power Systems (PMAPS)*, 2022. doi: 10.1109/PMAPS53380.2022.9810623 pp. 1–6. [Pages 10 and 11.]
- [16] X. Liu, J. Liu, Y. Zhao, T. Ding, X. Liu, and J. Liu, “A bayesian deep learning-based probabilistic risk assessment and early-warning model for power systems considering meteorological conditions,” *IEEE Transactions on Industrial Informatics*, vol. 20, no. 2, pp. 1516–1527, 2024. doi: 10.1109/TII.2023.3278873 [Pages 10 and 11.]
- [17] V. H. Chalishazar, J. Westman, J. Deines, S. Datta, J. Tagestad, A. Coleman, E. Barrett, M. Hoffman, A. Somani, and J. G. Schaad, “Wildfire risk evaluation framework for grid operations and planning,” in *2023 IEEE Power Energy Society General Meeting (PESGM)*, 2023. doi: 10.1109/PESGM52003.2023.10252841 pp. 1–5. [Pages 10 and 11.]
- [18] E. Ciapessoni, D. Cirio, S. Massucco, A. Pitto, and F. Silvestro, “A probabilistic risk assessment approach to support the operation of large electric power systems,” in *2009 IEEE/PES Power Systems Conference and Exposition*, 2009. doi: 10.1109/PSCE.2009.4840260 pp. 1–8. [Pages 10 and 11.]
- [19] L. Tang, Y. Lin, C. Hu, and L. Ma, “Risk status assessment of transmission lines based on big data platform,” in *2023 IEEE 6th Information Technology, Networking, Electronic and Automation Control Conference (ITNEC)*, vol. 6, 2023. doi: 10.1109/ITNEC56291.2023.10082079 pp. 1344–1347. [Page 10.]
- [20] A. Pan, X. Fang, Z. Yan, Z. Dong, X. Xu, and H. Wang, “Risk-based power system resilience assessment considering the impacts of hurricanes,” in *2022 IEEE/IAS Industrial and Commercial Power System Asia (ICPS Asia)*, 2022. doi: 10.1109/ICPSAsia55496.2022.9949709 pp. 1714–1718. [Pages 10 and 11.]

- [21] H. Hersbach, B. Bell, P. Berrisford, G. Biavati, A. Horányi, J. Muñoz Sabater, J. Nicolas, C. Peubey, R. Radu, I. Rozum, D. Schepers, A. Simmons, C. Soci, D. Dee, and J.-N. Thépaut, “Era5 hourly data on single levels from 1940 to present,” 2023. [Online]. Available: <https://doi.org/10.24381/cds.adbb2d47> [Pages xi, 14, 15, 16, and 50.]
- [22] J. Joyce, “Bayes’ theorem,” <https://plato.stanford.edu/archives/fall2021/entries/bayes-theorem/>, 2021, the Stanford Encyclopedia of Philosophy (Fall 2021 Edition), Edward N. Zalta (ed.). [Online]. Available: <https://plato.stanford.edu/archives/fall2021/entries/bayes-theorem/> [Page 23.]
- [23] A. O. Eggen, J. Heggset, K. Sagen, C. Aabakken, B. T. Hjartsjø, E. A. Østingsen, and S. O. Gjerstad, “Fasit, the norwegian reliability data collection system - experiences and utilitarian values,” in *IET Conference Proceedings*, 2023. doi: 10.1049/icp.2023.1214 pp. 2243–2247. [Online]. Available: <https://digital-library.theiet.org/content/conferences/10.1049/icp.2023.1214> [Page 26.]
- [24] G. W. Brier, “Verification of forecasts expressed in terms of probability,” *Monthly Weather Review*, vol. 78, no. 1, pp. 1–3, 1950. doi: 10.1175/1520-0493(1950)078<0001:VOFEIT>2.0.CO;2. [Online]. Available: [http://dx.doi.org/10.1175/1520-0493\(1950\)078<0001:VOFEIT>2.0.CO;2](http://dx.doi.org/10.1175/1520-0493(1950)078<0001:VOFEIT>2.0.CO;2) [Pages 30 and 31.]

